



REVIEW

High-intensity lasers and research activities in China

Yutong Li^{1,2,3,†}, Liming Chen⁴, Min Chen⁴, Feng Liu⁴, Yuqiu Gu⁵, Bing Guo⁶, Jianfei Hua⁷, Taiwu Huang⁸, Yuxin Leng⁹, Fei Li⁷, Lu Li⁸, Ruxin Li^{9,10}, Chen Lin^{11,12,13}, Wei Lu^{7,14,15}, Zhihui Lyu¹⁶, Wenjun Ma^{11,12,13}, Xiaonan Ning¹⁵, Yujie Peng⁹, Yang Wan¹⁷, Jinguang Wang¹, Zhaohua Wang¹, Zhiyi Wei¹, Xueqing Yan^{11,12,13}, Jie Zhang^{4,18}, Baozhen Zhao⁶, Zengxiu Zhao¹⁶, Cangtao Zhou⁸, Kainan Zhou⁵, Weimin Zhou⁵, Jianqiang Zhu¹⁹, and Ping Zhu¹⁹

¹Beijing National Laboratory for Condensed Matter Physics, Institute of Physics, Chinese Academy of Sciences, Beijing, China

²School of Physical Sciences, University of Chinese Academy of Sciences, Beijing, China

³Songshan Lake Materials Laboratory, Dongguan, China

⁴Key Laboratory for Laser Plasmas (Ministry of Education), School of Physics and Astronomy, Shanghai Jiao Tong University, Shanghai, China

⁵Research Center of Laser Fusion, Chinese Academy of Engineering Physics, Mianyang, China

⁶High-Intensity Laser and Particle Beam Laboratory, Department of Nuclear Physics, China Institute of Atomic Energy, Beijing, China

⁷Department of Engineering Physics, Tsinghua University, Beijing, China

⁸Center for Intense Laser Application Technology, and College of Engineering Physics, Shenzhen Technology University, Shenzhen, China

⁹State Key Laboratory of High Field Laser Physics, Shanghai Institute of Optics and Fine Mechanics, Chinese Academy of Sciences, Shanghai, China

¹⁰ShanghaiTech University, Shanghai, China

¹¹State Key Laboratory of Nuclear Physics and Technology, School of Physics, Peking University, Beijing, China

¹²Beijing Laser Acceleration Innovation Center, Beijing, China

¹³Institute of Guangdong Laser Plasma Technology, Guangzhou, China

¹⁴Institute of High Energy Physics, Chinese Academy of Sciences, Beijing, China

¹⁵Beijing Academy of Quantum Information Science, Beijing, China

¹⁶Human Key Laboratory of Extreme Matter and Applications, National University of Defense Technology, Changsha, China

¹⁷School of Physics, Zhengzhou University, Zhengzhou, China

¹⁸Tsung-Dao Lee Institute, Shanghai Jiao Tong University, Shanghai, China

¹⁹National Laboratory on High Power Laser and Physics, Shanghai Institute of Optics and Fine Mechanics, Chinese Academy of Sciences, Shanghai, China

(Received 21 May 2024; revised 11 September 2024; accepted 29 September 2024)

Abstract

This paper provides an overview of the current status of ultrafast and ultra-intense lasers with peak powers exceeding 100 TW and examines the research activities in high-energy-density physics within China. Currently, 10 high-intensity lasers with powers over 100 TW are operational, and about 10 additional lasers are being constructed at various institutes and universities. These facilities operate either independently or are combined with one another, thereby offering substantial support for both Chinese and international research and development efforts in high-energy-density physics.

Keywords: high-energy-density physics; high intensity; ultrafast and ultra-intense lasers

1. Introduction

Parameters such as the duration, energy, power and wavelength are commonly utilized to characterize laser pulses. The development trend in laser technology aims to overcome the limitations of these parameters. Laser pulse durations

Correspondence to: Y. Li, Beijing National Laboratory for Condensed Matter Physics, Institute of Physics, Chinese Academy of Sciences, Beijing 100190, China. Email: ytli@iphy.ac.cn

[†]The author names are sorted according to Chinese Pinyin of the surname except the first author.

have been shortened to the attosecond scale, and pulse energy has increased to megajoule levels. Various scientific studies and applications can be conducted using various lasers.

Based on the pulse duration and energy characteristics, facilities utilizing intense lasers for high-energy-density physics research can be categorized into two distinct types. The first type comprises high-energy lasers that typically operate over a duration of several nanoseconds and produce output pulse energies ranging from kilojoules to megajoules (kJ–MJ). An exemplary high-energy laser system is the National Ignition Facility (NIF), constructed at the Lawrence Livermore National Laboratory (LLNL). This facility can deliver approximately 2.0 MJ at 3ω within 5–10 ns using 192 laser beams^[1]. The second category encompasses high-intensity lasers, which primarily utilize the chirped-pulse amplification (CPA) technique, invented by Strickland and Mourou in 1985^[2]. This technique allows the compression of laser pulses to femtosecond or picosecond scales, significantly enhancing the peak power of the lasers. Although these lasers have relatively lower pulse energy than their high-energy counterparts, their ability of the highly focused intensity on the target surface due to the short pulse duration categorizes them as ultrafast and ultra-intense lasers.

In recent decades, China has achieved remarkable progress in developing both categories of laser technologies. Facilities such as Shenguang I (SG-I), Shenguang II (SG-II) and Shenguang II upgrade (SG-II U) with a petawatt (PW) picosecond beam have been established in Shanghai. The recent upgrades to the SG-II U facility have doubled its energy output and added an additional picosecond PW beam. Moreover, a laser facility capable of 100-kJ-level outputs and its prototype have been constructed in Mianyang^[3]. These advanced high-energy lasers are predominantly employed for exploring inertial confinement fusion (ICF), laboratory astrophysics and other processes related to high-energy-density physics.

Numerous institutions and universities across China have developed or are in the process of constructing ultrafast and ultra-intense laser facilities, with peak powers spanning from terawatts (TW) to 100 PW. The Shanghai Institute of Optics and Fine Mechanics (SIOM) of the Chinese Academy of Sciences (CAS), the Research Centre for Laser Fusion of the China Academy of Engineering Physics in Mianyang and the Institute of Physics (IOP) of the CAS in Beijing were among the first to initiate the construction and research of these sophisticated laser systems. Over the years, other prominent institutions such as Shanghai Jiao Tong University (SJTU), Peking University (PKU), Tsinghua University, Chinese Academy of Atomic Energy, National University of Defense Technology (NUDT) and Shenzhen Technology University (SZTU) have joined this field. These ultrafast facilities are primarily engaged in

physics and application research in areas including laser-driven electron acceleration, ion acceleration, ultrafast X-ray emission, terahertz radiation and laser nuclear physics.

In recent years, there has been a surge in the establishment of ultrafast laser facilities and laboratories across various disciplines. However, this study does not encompass all these developments. Consequently, our review will focus predominantly on those ultrafast high-intensity laser facilities boasting peak powers exceeding 100 TW and the associated research activities in high-energy-density physics that utilize these facilities.

2. Main laser facilities and research activities in China

This section presents an overview of the intensive laser facilities and related research activities in high-energy-density physics, organized by geographic distribution across Beijing, Shanghai and other areas.

2.1. Institute of Physics, Chinese Academy of Sciences

In 1995, the Optical Physics Laboratory of the IOP, CAS in Beijing, commissioned a femtosecond laser system. This system, characterized by a pulse energy of 5 mJ, pulse duration of 120 fs, wavelength of 800 nm and repetition rate of 10 Hz, represented the first-generation femtosecond laser from spectra-physics, utilizing an argon-ion pump laser. Relying on this laser, the IOP started to study ultrafast intense laser–plasma interaction physics, and made advancements in the generation of hard X-rays and hot electrons^[4–6].

Since 1997, the team at the IOP has been engaged in the independent development of femtosecond lasers, successively establishing the Xtreme Light (XL-I)-I, XL-II and XL-III Ti:sapphire systems. The XL-I system was completed in 1999, delivering an output of 36 mJ over 25 fs at a repetition rate of 10 Hz. The beam quality surpassed four times the diffraction limit^[7]. The focal spot size, as determined by an X-ray pinhole camera, was approximately 10 μm , achieving focused intensities on targets of 1×10^{17} W/cm². The pulse contrast at 1 ps exceeded 10^5 , as measured using a third-order autocorrelator.

In contrast to XL-I, the XL-II laser system, constructed in 2001, incorporated a regenerative amplifier for pre-amplification to enhance beam quality^[8]. An image-transfer system in vacuum was utilized to project the near-field modes of the pump laser onto the amplifying crystal, improving both the pump efficiency and the post-amplification beam quality. Stretchers and compressors equipped with gratings of varying densities were employed to offset high-order dispersion. This system produced a laser output of 644 mJ at 33 fs, corresponding to a peak power of approximately 20 TW. The beam quality was three times

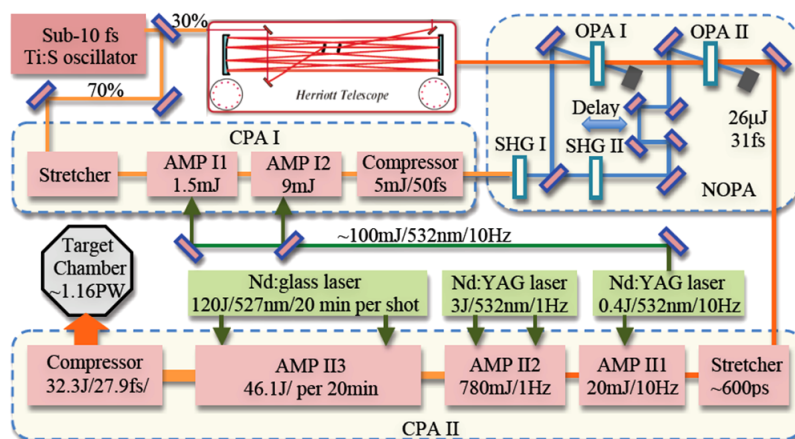


Figure 1. Layout of the XL-III laser system^[9].

the diffraction limit, with the focused intensity approaching 10^{19} W/cm².

In 2006, the team developed the XL-III femtosecond laser, achieving a peak power of 350 TW, and subsequently upgraded this system to the petawatt level in 2011^[9]. Figure 1 shows the layout of the XL-III laser system. A sub-10 fs Ti:sapphire laser oscillator was designed to serve as the seed source. By integrating femtosecond optical-parametric amplification (fs-OPA) with double-chirped-pulse amplification (DCPA), the contrast ratio was enhanced to 10^{10} . The laser output reached 32.3 J at a duration of 27.9 fs, corresponding to a peak power of 1.16 PW, making it the highest output for Ti:sapphire laser systems at that time.

In 2012, the IOP constructed a new experimental building and relocated the XL-III laser facility and the team to a new laboratory within this structure. In addition, a 20 TW femtosecond laser provided by Amplitude of France was installed. A new experimental target area was established within a year, further enhancing the facility's capabilities.

Since 2018, the IOP has been developing the National Research Infrastructure, known as the Synergetic Extreme Condition User Facility (SECUF), situated in Huairou District, Beijing. The SECUF provides extreme experimental conditions – including exceptionally low temperatures, strong magnetic fields, ultra-high pressures and ultrafast light fields – for both Chinese and international researchers to engage in pioneering research in materials science. The facility commenced operations in early 2023. Within the SECUF, the team constructs and manages two experimental platforms: the ultrafast X-ray dynamics platform, driven by a PW laser system, and the ultrafast electron diffraction (UED) platform, driven by a kHz fs laser system.

The Huairou PW laser system and the ultrafast X-ray dynamics platform are primarily designed to offer ultra-intense light fields and laser-driven ultrafast X-rays for studying material dynamics and high-energy-density physics. Figure 2 illustrates the layout of the Huairou

PW laser system and its target areas. The design of the laser system was a collaborative effort between Amplitude and the IOP and was implemented by Amplitude. It is a dual-arm system, featuring a PW (25 J, 25 fs, 800 nm) arm capable of operating at one shot per minute, and a secondary 3 TW (60 mJ, 20 fs, 800 nm) arm that operates at 100 Hz. Both arms utilize a common high-contrast front-end based on double CPA, as well as a cross-polarized wave (XPW) system that significantly enhances pulse contrast, measured to be 2.5×10^{10} @200 ps. The system demonstrates exemplary performance in pulse spatiotemporal characterization and stability, thanks to various active control systems including the automatic beam alignment system, programmable acousto-optic spectral gain controller Mazzler, Dazzler–Wizzler feedback and laser adaptive optics (AO) system.

The PW arm is designed to deliver pulses to various target chambers, enabling a spectrum of high-energy-density physics experiments. These experiments include laser wake-field acceleration (LWFA), generation of ultrafast X-ray sources, interactions between lasers and clusters, the use of near-critical density (NCD) gas targets, laser-driven nuclear physics and the production of novel THz radiation. The resulting X-ray emissions act as probes to study the dynamics of different samples in a single shot.

In the 3 TW arm, laser pulses are focused onto tape- or disk-shaped targets to generate K-alpha X-ray emissions at a 100 Hz repetition rate with a high average flux. This configuration is ideal for high spatial resolution imaging and ultrafast X-ray diffraction. The photon fluxes of Cu K α (~8.04 keV) and Mo K α (~17.44 keV) measured are 1.7×10^{11} and 7.5×10^{10} photons/s, respectively. By varying the target materials, different X-ray photon energies can be achieved. This platform facilitates the synchronous integration of fs laser pulses, X-rays and THz sources to explore the ultrafast dynamics of matter using various pump-probe schemes, such as fs laser/THz pumps followed by fs laser/THz/X-ray probes.

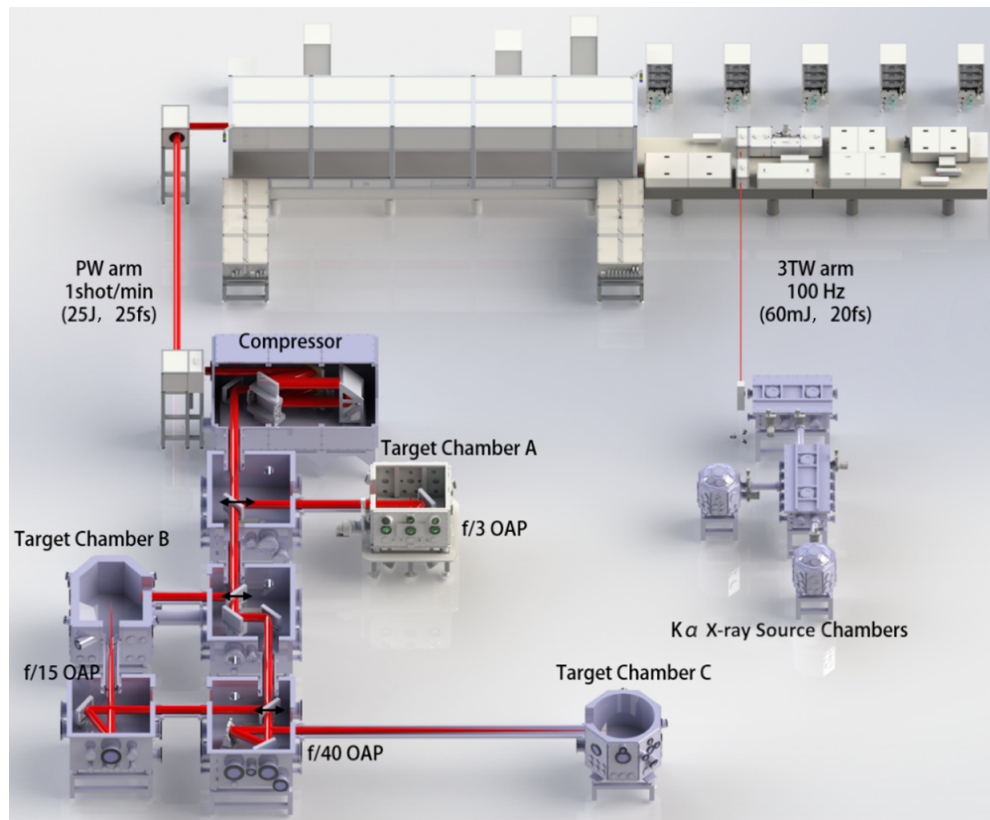


Figure 2. Layout of the Huairou PW laser and target areas. Target Chamber A with $f/3$ off-axis parabola (OAP) is used to study novel THz radiation. Target Chamber B with $f/4$ and $f/15$ OAPs is used to study interactions between the laser and cluster or near-critical density gas targets and laser-driven nuclear physics. Target Chamber C equipped with an $f/40$ OAP is used for studying laser wakefield acceleration and associated X-ray sources. The 3 TW/100 Hz beamline is for ultrafast X-ray and THz generation and applications.

Research activities of the IOP team

The IOP team has primarily focused on investigating alternative ignition schemes for ICF, the production of intense laser-driven X-ray and THz radiation and laboratory astrophysics.

Fundamental to the fast ignition (FI) approach to ICF and the creation of secondary particles and radiation sources is the generation of fast electrons during intense laser–plasma interactions. The team has studied the characteristics of fast electrons, including their generation mechanisms, spatial and energy distributions, dynamics and transport in dense plasmas, as well as their dependency on laser and target parameters. For instance, they observed a collimated fast electron beam emitted along the front target surface at large laser incidence angles^[10] owing to the confinement effects of surface magnetic and electrostatic fields. To address the issue of large divergence angles of fast electron propagation in the high-density plasma core relevant to FI, they demonstrated that laser-to-core coupling efficiency could exceed 10% when a multi-megagauss magnetic field was used to guide fast electrons in particle-in-cell (PIC) simulations^[11]. They also showed that such a magnetic field can be generated using an open-ended coil^[12] or a capacitor-coil target^[13,14] driven by high-power lasers. Based on these findings, Zhang

et al.^[15] proposed a double-cone ignition (DCI) scheme for ICF that encompasses four processes: quasi-isentropic compression, acceleration, head-on collision and rapid heating. Their experiments confirmed the feasibility of this scheme at current energy levels^[16].

The generation of high-intensity and broadband THz radiation sources presents significant challenges in advancing THz science. Our team has been exploring the production of THz radiation using relativistic ($>10^{18}$ W/cm²) laser pulses interacting with high-density plasma targets^[17]. They discovered that coherent transition radiation, emitted by fast electrons escaping from the rear side of a laser-irradiated foil, could yield strong THz radiation^[18]. In collaboration with scientists in the UK, they achieved extreme THz radiation with pulse energies up to approximately 200 mJ and unprecedented terawatt-level peak power by optimizing THz generation efficiency at the VULCAN laser facility^[19,20]. Recently, the team utilized THz radiation as a diagnostic tool to observe the dynamics of fast electrons, finding that the electron pulses could be as brief as the driving duration of the femtosecond laser pulses^[21].

In collaboration with colleagues from the National Astronomical Observatory, Beijing Normal University, SJTU and other institutions, the team has been investigating magnetic

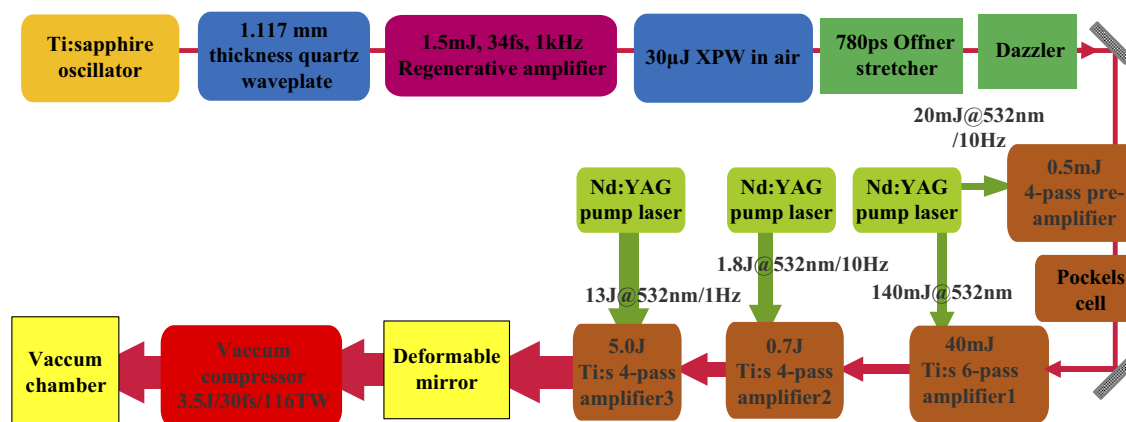


Figure 3. Layout of the 100 TW laser system.

reconnection (MR), collisionless shocks, jets and other topics in laboratory astrophysics at the SG laser facility. In their MR studies, they demonstrated that the MR topology produced in high-power laser–plasma interactions in the laboratory closely resembles the loop-top-like X-ray source emissions observed in solar flares^[22]. More recently, they observed turbulent MR characterized by fragmented current sheets, multiple magnetic islands and fluxtubes using optical shadowgraphy^[23]. For collisionless shocks studies, they demonstrated a supersonic plasma collision scheme driven by intense laser pulses to generate collisionless shock waves, and observed their dynamic evolution process^[24].

2.2. China Institute of Atomic Energy

Since 2017, the China Institute of Atomic Energy (CIAE) team has been developing a 100 TW laser system. By 2020, the final output achieved was 3.5 J at 35 fs and 1 Hz^[25]. The pulse duration was further refined to 30 fs using Dazzler and Wizzler loops. The laser beam wavefront, after being directed through an off-axis parabola with a 1.2 m focal length, was corrected using a deformable mirror and SID4 sensor feedback system, resulting in a Strehl ratio of 0.85 and a focal spot size (full width at half maximum, FWHM) of 20 μm .

Using an off-axis parabola with a 350 mm focal length, the focal spot could reach approximately 7 μm (FWHM). Owing to the implementation of double CPA, XPW generation in air and Pockels cells, the measured temporal contrast was 6.5×10^{10} . Consequently, the peak power of the final output reached 116 TW (3.5 J/30 fs at 1 Hz), with an energy stability of 0.65% root mean square (RMS). This configuration is illustrated in Figure 3.

To generate a broadband XPW signal, a multi-order waveplate with a thickness of 0.117 mm was positioned before the regenerative amplifier to reduce the gain-narrowing effect, and the measured spectrum of the XPW was 68 nm (FWHM)^[26]. A pinhole was used in the XPW

system to improve the energy stability^[27]. To refine the amplified beam profile, the pump beams of the pre-amplifier and first amplifier were projected onto the Ti:sapphire crystal from the exit of the pump laser in air, on both sides of the crystal. The pump beams for the second amplifier were directed onto a Ti:sapphire crystal within a vacuum chamber. The pump beam profiles for the final amplifier were homogenized using a diffractive optical element (DOE) plate.

Research activities of the CIAE team

The CIAE team has primarily focused its research on laser wakefield electron acceleration, laser-driven proton acceleration, fast neutron generation, laser-driven THz generation and laser nuclear physics^[28].

The supersonic gas target is a key element in laser wakefield electron acceleration. The team has systematically conducted simulations and experimental studies on gas targets customized for laser accelerators. A Nomarski optical interference system with high spatial-temporal resolution (6 μm , 6 ns) was set up to diagnose gas density^[29]. The team has developed supersonic gas targets with various structures and investigated the impact of multiple parameters on the gas jet performance^[30]. To accurately measure the electron beams, the team designed multiple electron magnetic spectrometers covering different energy ranges and systematically studied the characteristics of imaging plate (IP) plate detectors^[31]. Currently, the team has generated a high-energy electron beam (200 MeV, ~ 50 pC) using a gas target.

For laser-driven proton acceleration, the team has proposed schemes based on target normal sheath acceleration (TNSA) and radiation pressure acceleration (RPA), assisted by an external axial magnetic field. These schemes are designed to accelerate and collimate protons when a right-hand circularly polarized laser irradiates an over-dense plasma and a multispecies nanofoil^[32,33]. For fast neutron generation, the team has proposed the irradiation of a multichannel target consisting of a row of parallel microwires

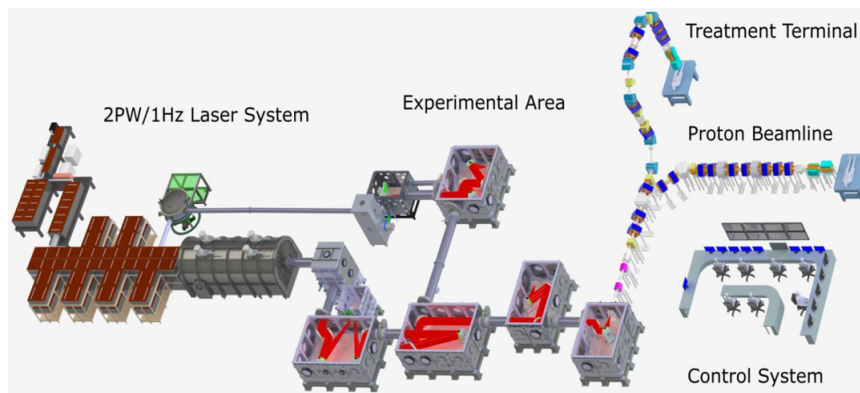


Figure 4. Layout of CLAPA-II.

and a plane substrate with a relativistic femtosecond laser to enhance neutron yields^[34].

The team has also developed a scheme based on the interaction between a relativistic femtosecond-intense laser and a T-shaped target to generate ultrafast terahertz radiation. The results demonstrated that T-shaped targets can increase the terahertz radiation intensity by an order of magnitude, achieving up to 2.8 TV/m, compared to 0.3 TV/m for planar targets. In addition, the cone angle of the collimated terahertz beam was reduced by approximately six times^[35,36]. The team further proposed enhancing terahertz radiation through a double-layer target configuration consisting of ‘NCD plus solid’ layers, which showed that the peak electric field was more than five times greater than that of single-layer targets^[37].

The dynamics of nuclear reactions in laser-driven plasma environments, including astrophysical reactions and the ICF design, are critically important in laser nuclear physics research^[38]. The team has developed a direct calibration method using a gated fission neutron source from ²⁵²Cf to accurately calibrate neutron detectors for experiments involving laser-driven nuclear reactions^[39].

2.3. Peking University

At the Beijing Laser Acceleration Innovation Center (BLAIC) at PKU, funded by the Ministry of Science and Technology, a team is constructing a proton tumor therapy system powered by a petawatt femtosecond laser. The central component of this system is the laser-driven proton accelerator, CLAPA-II, which utilizes a transient ultra-strong electrostatic field generated by the interaction of an ultra-high-intensity laser with high-density targets to accelerate protons^[40,41]. This accelerator is equipped with a dedicated beam transport system that collects protons and precisely controls the energy and flux of the beam. At the treatment terminal, the treatment head adjusts the shape and energy spectrum of the proton beam to deliver the required radiation dose to the tumor according to the prescribed treatment plan.

The predecessor of CLAPA-II, CLAPA-I, was completed by our team in 2018. It employed a 200 TW Ti:sapphire laser as the driving source and was capable of generating monoenergetic protons with energies ranging from 1 to 15 MeV, achieving an energy spread of 1% and a flux of 10^6 – 10^8 per shot^[42–44]. At CLAPA-I, the team gained extensive experience in various applications, including cell irradiation^[45–47].

The CLAPA-II laser, developed collaboratively by PKU and Thales, can achieve dual-beam outputs of 2 and 200 TW, as shown in Figure 4. Specifically, the 2 PW laser delivered a pulse with a duration of 30 fs and a peak energy of 60 J. This system is based on a double CPA architecture using Ti:sapphire amplifiers and employs a hybrid technique of XPW and optical-parametric chirped-pulse amplification (OPCPA) to achieve temporal contrast in the area of 10^{13} @ 100 ps. To meet the requirements of tumor treatment, the laser operates at a repetition rate of 1 Hz with a 300 mm beam diameter at FWHM. The integration of a large-aperture AO system allows for effective correction of wavefront phase aberrations, resulting in a Strehl ratio better than 0.85 after correction.

Once the laser reaches the target area, its contrast is further enhanced by a dual-plasma mirror (PM) system. High-contrast laser pulses, once focused by an off-axis parabolic (OAP) mirror, are anticipated to achieve peak intensities exceeding 10^{22} W/cm². Early theoretical and experimental results have indicated that utilizing nanometer-thick film targets^[48,49] or composite targets^[50] at such high intensities is highly promising for generating protons exceeding 100 MeV, with an adequate flux for tumor therapy^[51,52]. Treating a tumor effectively requires hundreds of shots at a frequency of 1 Hz, with each target being completely destroyed during its interaction with the laser. Therefore, the target system in the laser accelerator must continuously supply high-quality targets at the laser firing rate, ensuring that the position of newly positioned targets does not deviate by more than a few micrometers. Currently, researchers at the BLAIC have developed a high-repetition-rate target system capable

of accommodating various types of targets, including solid film^[53], liquid film^[54], free-standing and composite carbon nanotube targets^[49,55–58]. A debris shield system has also been designed to protect the OAP mirror and other valuable optical components from contamination.

Directly behind the targets, CLAPA-II uses three superconducting solenoids to collect the diverging laser-accelerated protons. After collection, the quasi-parallel beam is directed to either a horizontal or vertical achromatic beam transmission segment for energy selection^[59]. Notably, in the vertical segment, superconducting canted-cosine-theta (CCT) magnets are employed to generate both dipole and quadrupole magnetic fields, significantly reducing the weight and complexity of the apparatus.

The overall control system of the proton therapy unit operates on the Experimental Physics and Industrial Control System (EPICS) software platform, a distributed control system that enables time-synchronized control of the laser, target area, beam transport system and treatment terminals with comprehensive safety interlock control functions^[6]. The treatment planning system, based on Monte Carlo algorithms, generates treatment plans tailored to the characteristics of the laser-accelerated beam, ensuring the effective use of protons generated by laser acceleration to safely irradiate tumor tissue while sparing healthy tissue.

The installation of the CLAPA-II laser is now completed, and it is currently undergoing testing and commissioning. The construction of the target area and the horizontal beam transport system has also been finalized, with experiments projected to commence by 2024.

2.4. Tsinghua University/Beijing Academy of Quantum Information Sciences/Institute of High Energy Physics, Chinese Academy of Sciences, 1 Hz 30 fs 1 PW system

2.4.1. 1 Hz 30 fs 1 PW system

In collaboration with Tsinghua University and with the support of the Beijing government, Beijing Academy of Quantum Information Sciences (BAQIS) has developed a compact 1 Hz, 30 fs, 1 PW Ti:sapphire laser system. This system features high-contrast front-ends using the XPW scheme and multi-stage Ti:sapphire amplifiers, achieving an energy output of approximately 47 J before compression. The compressed pulse possesses a peak power exceeding 1 PW and a pulse width of less than 30 fs. The typical parameters are detailed in Table 1. The system's modular design incorporates industrial-grade lasers in a compact structure. Compared to commercial PW laser systems, its footprint is reduced by a factor of three, resulting in exceptional long-term stability.

Figure 5 illustrates the PW laser system, comprising several independent modules: a femtosecond oscillator, CPA1,

Table 1. Typical parameters of a PW laser system.

Parameters	Values
Wavelength	~800 nm
Energy (post-compression)	> 30 J
Pulse duration	<30 fs (FWHM)
Repetition rate	1 Hz
Picosecond contrast	> 10 ¹⁰ @100 ps
Pulse energy stability	<0.5% (RMS, 8 h)

CPA2, XPW contrast booster, 20 TW amplifier, 200 TW amplifier, PW amplifier, test compressor and pump lasers. The seeding source utilizes an 800 nm@80 MHz femtosecond oscillator with a 100 nm bandwidth and 200 mW average power. The high-contrast front-end amplifier employs a double CPA design coupled with an XPW contrast booster. Initially, the seeding pulse is amplified in CPA1 to a few millijoules, compressed to 30 fs, then enhanced for pulse contrast via the XPW model, and further amplified in CPA2 to reach 10 mJ. The pulse subsequently passes through the 20 and 200 TW multi-pass amplifiers, achieving a pulse energy of 7 J. The final PW amplifier boosts the pulse energy to over 47 J, with the pulse then being compressed to less than 30 fs, resulting in a peak power exceeding 1 PW. The primary pumping sources for the 200 TW and PW amplifiers are compact high-energy neodymium-doped yttrium aluminum garnet (Nd:YAG) lasers (8–15 J at 532 nm) operating at 1 Hz, with potential for upgrading to 5 Hz. An integrated monitoring system has been developed to monitor and control the operating status and environmental parameters of each module, including the spectrum, energy, beam profile, temperature and humidity.

In 2023, a collaboration between BAQIS, Tsinghua University and the Institute of High Energy Physics (IHEP) of the CAS was initiated to establish an advanced research platform for plasma wakefield acceleration (PWFA). This platform, situated in the #10 experimental hall of the IHEP, integrates the PW laser system, the 2 GeV BEPC-II electron and positron linac (Beamline-I) and a new 150 MeV high-charge electron linear accelerator (linac; Beamline-II). The PW laser can be combined with Beamline-I's linac to investigate LWFA with external injection of both electron and positron beams. Beamline-I and Beamline-II are designed to merge collinearly at a focal point through a dogleg configuration. This setup, utilizing the 2 GeV electron/positron beams from Beamline-I and the low-emittance high-charge electron beams from Beamline-II, facilitates a variety of experimental studies related to LWFA and PWFA. The research focus of this platform includes critical physics issues in LWFA and PWFA, such as enhancing beam quality, boosting acceleration efficiency and suppressing various instabilities. In addition, utilizing the unique positron beam from BEPC-II, the platform will conduct pioneering research on high-quality positron acceleration in PWFA and LWFA.

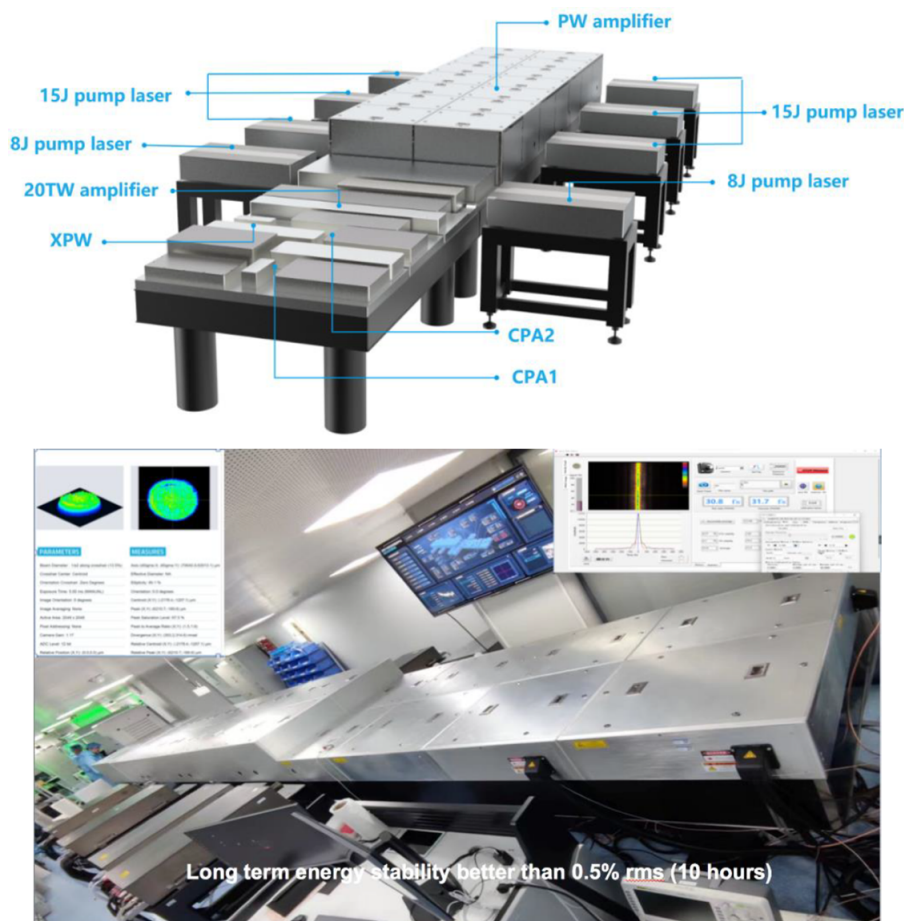


Figure 5. BAQIS–Tsinghua 1 PW laser system.

2.4.2. Fudan-BAQIS-Tsinghua 3 Hz 300 TW laser system and ICS

Since 2023, Fudan University, BAQIS and Tsinghua University have also collaborated to develop a compact MeV-level inverse Compton scattering (ICS) source for nuclear photonics research. This ICS platform is driven by a 25 fs, 3 Hz, 300 TW high-power laser, employing the same technology as the aforementioned PW laser system. Detailed parameters of this system are listed in Table 2.

Table 2. Typical parameters of a 300 TW laser system.

Parameters	Values
Wavelength	~800 nm
Energy (post-compression)	> 8 J
Pulse duration	<25 fs (FWHM)
Repetition rate	≥3 Hz
Contrast	> 10 ¹⁰ @100 ps
Pulse energy stability	<1.0% (RMS, 1 h)
Pointing jitter	<1.0 μrad (RMS, 8 h)
Beam size	~100 mm (1/e ²)

The MeV-level ICS source employs a dual-beam collision scheme, as illustrated in Figure 6. The primary advantage of this scheme is its capability to independently adjust the parameters of the two laser beams to optimize the ICS gamma-ray output. In this setup, the 300 TW ultra-intense laser pulse is divided into two beams: a 200 TW beam is focused and directed into the main target chamber to drive LWFA, while the 100 TW scattered laser beam is focused to collide with the LWFA electron beam at an angle of approximately 170°. This collision generates MeV-level ICS gamma rays with a single-shot photon flux exceeding 1.5×10^8 . The system comprises several modules, including a laser compression/splitting module, a plasma source generation/control module, an optical diagnostic module for plasma structure, a laser transmission/control module, a laser focusing module, an electron beam energy spectrometer, a shielding module and other synergistic subsystems. Through its monitoring and control modules, the system provides comprehensive control over the generation, tuning and diagnostics of ICS gamma rays, creating a flexible and versatile experimental environment for various applications.

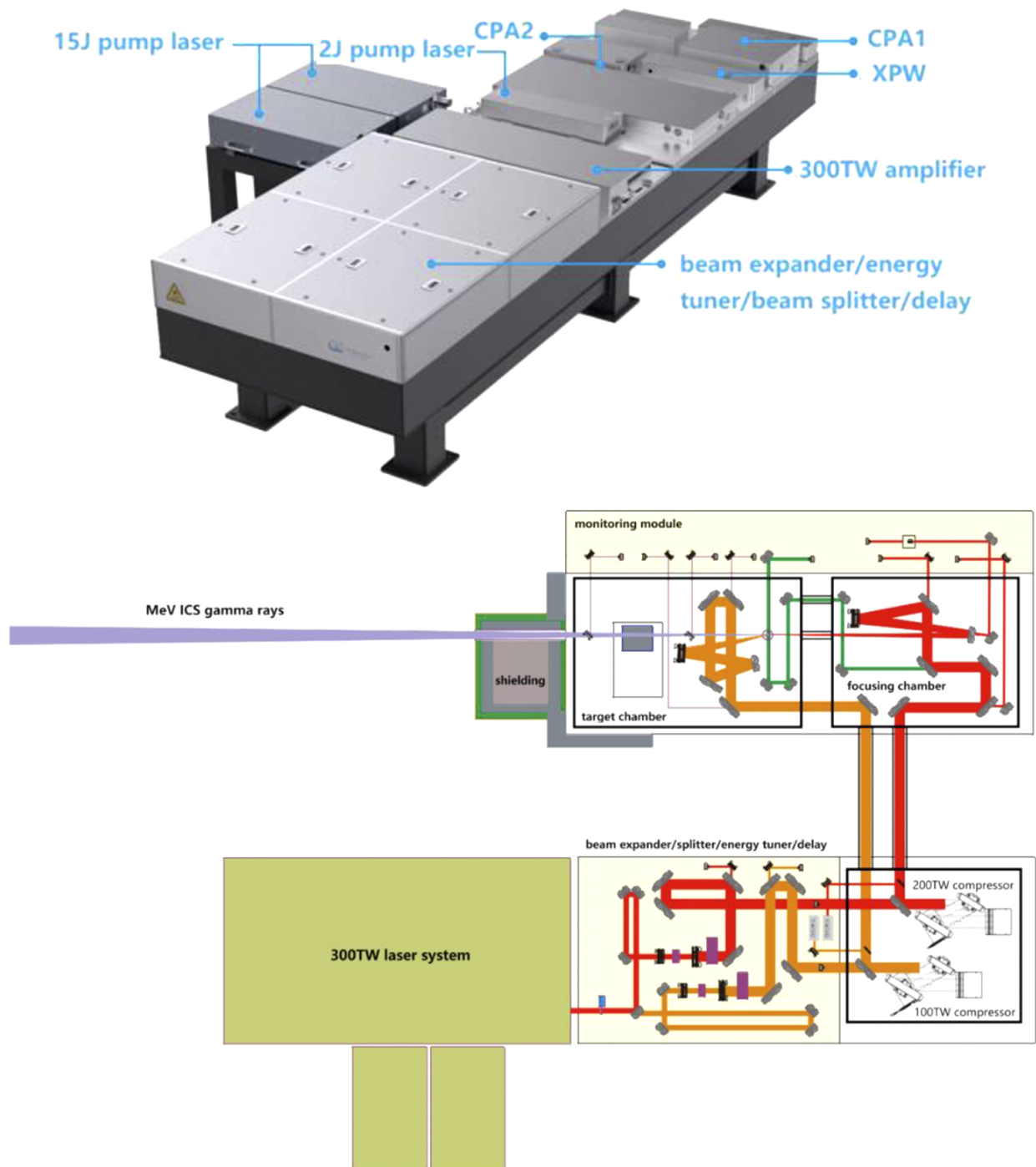


Figure 6. Layout of the Fudan-BAQIS-Tsinghua 300 TW laser system and the MeV ICS source.

2.4.3. ‘Zhongyuan Light’: the Zhengzhou University-Tsinghua joint laser accelerator facility for application

In 2023, the first medium-scale scientific facility in Henan, China, named ‘Zhongyuan Light’, was officially approved, and construction commenced. Jointly designed by Tsinghua University and Zhengzhou University, this facility aims to build a laser-plasma accelerator for end-users across diverse

research fields by utilizing the latest domestically developed compact robust ultrashort high-power laser technology. The facility will feature approximately 10 independent beamlines, including a compact petawatt laser system, PW laser-driven high-energy high-quality electron acceleration, proton acceleration and application, a test platform for LWFA-driven free electron lasers, a betatron radiation source, an ICS source, a single-cycle intense mid-infrared



Figure 7. Layout of Zhongyuan Light.

source, and an UED platform. Figure 7 depicts the layout of these beamlines. The construction plan spans five years, with seven beamlines expected to be operational and available for users within approximately three years.

Research activities of Tsinghua team

The laser–plasma accelerator group at Tsinghua University has been dedicated to advancing laser–plasma acceleration technology (LWFA/PWFA) and its applications. The group has also actively engaged in developing compact ultrafast ultra-intense lasers for various applications through collaboration with BAQIS and the Qiyuan Institute of New-light Source in Kaifeng.

In LWFA/PWFA-related physics, the group has made significant progress on various topics, including the phase space dynamics of injection schemes^[60–63], ultra-high-brightness beam generation^[64–67], electron snapshots for plasma wake-field diagnostics^[68,69], positron acceleration^[70,71] and external injection^[72].

For high-brightness injection in LWFA/PWFA, various injection schemes^[63–66] have been proposed for generating high-quality beams with low emittance and low energy spread. In phase space dynamics, the origin of the phase space mismatch in plasma accelerators was analyzed^[61], and matching schemes were proposed to preserve beam emittance^[62]. In the phase space manipulation method, a hollow channel plasma is proposed to rotate the

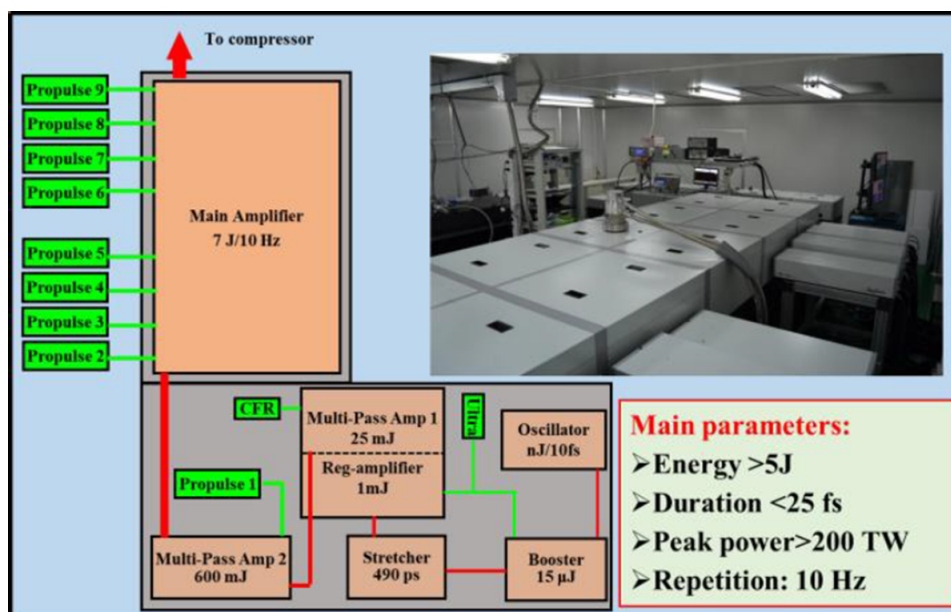


Figure 8. The 200 TW laser system at the LLP, SJTU.

beam longitudinal phase space^[60,73], reducing the beam energy spread (beam chirp) from approximately 1% to approximately 0.1%. For diagnostic development, a novel approach based on femtosecond electron beam snapshots was proposed to directly image linear and nonlinear plasma wakefield structures^[67,68]. Several novel schemes for high-quality positron acceleration and beam loading have been proposed^[69,70]. External injection from a linac to LWFA was demonstrated for the first time^[71].

Regarding the applications of plasma accelerators, the group has been focusing on several major applications of LWFA, including all-optical desktop X-ray and gamma-ray sources^[74–77] based on betatron and ICS schemes, MeV UED based on LWFA, intense mid-infrared source based on laser-plasma ‘photon deceleration’, high-energy electron therapy based on LWFA, etc. The group has successfully built the first true ‘table-top’ synchrotron light source based on betatron and ICS, demonstrated MeV UED based on LWFA^[78] and generated tunable 3–20 μm mJ near-single-cycle intense mid-infrared pulses^[79,80]. They have also developed a novel scheme for laser-driven ion acceleration^[81,82].

In collaboration with BAQIS and the Qiyuan Institute of Newlight Source in Kaifeng, the group has built the most compact and robust high-power lasers with peak powers ranging from 20 TW to 1 PW. These new laser systems are key to developing genuine ‘table-top’ light sources based on laser-plasma acceleration.

2.5. Shanghai Jiao Tong University

Two laboratories at SJTU have conducted studies on high-intensity laser-plasma interactions: the Key Laboratory for Laser Plasmas (LLP) and the Tsung-Dao Lee Institute

(TDLI). A 200 TW fs laser system was first installed at the LLP in 2012 and later relocated to a new building in the Department of Physics with upgraded performance. The TDLI was established in 2016, and a 2.5 PW fs laser is currently under construction.

2.5.1. Key Laboratory for Laser Plasmas

The 200 TW Ti:sapphire laser system, supplied by Amplitude of France, was installed at the LLP. It is the first 100-TW-level commercial laser system in China. A block diagram of the laser is shown in Figure 8. The 200 TW laser system was constructed based on the double CPA scheme. The first CPA system consisted of an oscillator and a contrast booster. Within the booster, the laser seed from the oscillator, operating at a repetition rate of 75 MHz, was amplified to the millijoule level, with the repetition rate reduced to 10 Hz. The amplified seed was cleaned using a saturable absorber to improve the amplified spontaneous emission (ASE) contrast. The seed was then sent to the second CPA system, which consists of a stretcher, a regenerative amplifier and three multi-pass amplifiers. Finally, an amplified 10 Hz infrared laser beam with a pulse energy of approximately 7 J was obtained in the main amplifier.

As shown in Figure 9, the laser pulse was compressed to a duration of 25 fs and an energy of 5 J in the compressor. The laser beam is then directed to two separate target chambers. In the solid-target chamber, the laser is focused by a short focal length OAP ($f/4$) onto solid targets for experiments such as ion acceleration, THz generation and relativistic high-order harmonic generation. In the gas target chamber, the laser is focused by a long focal length OAP ($f/18$) onto gas targets for experiments including laser wakefield electron acceleration and X-ray/ γ -ray generation.

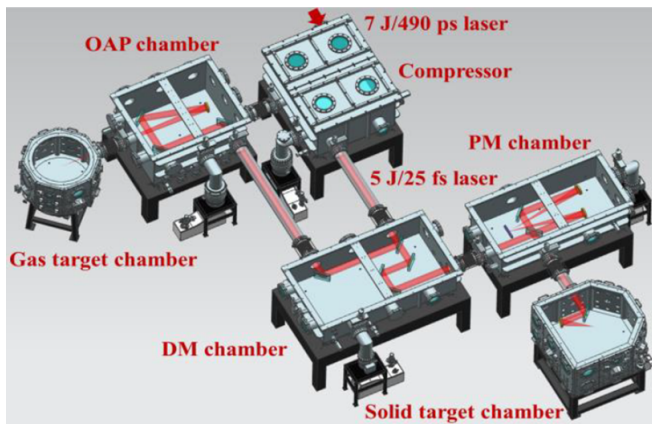


Figure 9. The experimental area at the LLP, SJTU.

In 2017, the contrast booster was upgraded by replacing the saturable absorber with an XPW unit, significantly improving the laser contrast. Combined with a PM developed by the SJTU team in the PM chamber^[83], the ASE contrast 10 ps before the main pulse improved by more than a factor of 10^{10} . This high contrast enables experiments that require very high laser contrast, such as the ion acceleration from thick foils and the generation of high-order harmonics from solid plasma surfaces.

After approximately 10 years of operation, the laser was further upgraded in 2023 to include two beamlines with peak powers of 200 and 300 TW, as shown in Figure 10. To enhance laser stability and performance, the pump lasers for the contrast booster and regenerative amplifier were replaced with diode-pumped Nd:YAG lasers. The laser repetition rate at the front-end was increased to 100 Hz. The main amplifier was upgraded to be compatible with a 500 TW, 1 Hz laser system.

The pulse energy at the main amplifier reached 18 J, which was then split into two beamlines with energies of 11 and 7 J. These beams were compressed in two separate compressors

to 25 fs simultaneously, achieving pulse energies of 7.5 and 5 J, respectively. With a delay time in the 200 TW beamline, the two beams were synchronized at the outputs of the compressors. The construction of this upgraded laser system is nearly completed, and it is scheduled to perform its first experiment in 2024.

After compression, the two beams were directed to the experimental area within a radiation-shielded room, as depicted in Figure 11. Two distinct interaction geometries were employed for the beams, primarily to facilitate interactions with gas targets. In the first interaction chamber, the beams converge at the interaction point at an obtuse angle to conduct experiments such as nonlinear Thomson scattering. In the second chamber, the beams converge at an acute angle, enabling experiments such as staged laser wakefield electron acceleration. The comprehensive system comprising the laser and target chambers is designated as the Chongming Laser Experimental Facility (CLEF), named after the mythical Chinese bird Chongming, noted for having two pupils in one eye.

Research activities of the SJTU-LLP team

The SJTU-LLP team has focused extensively on the interaction of femtosecond lasers with plasma for particle acceleration, radiation generation and various applications.

The objective of particle acceleration is to produce high-quality, high-energy electron beams via LWFA. Several ionization injection techniques have been explored and implemented^[84–87]. A quasi-monoenergetic GeV-level electron beam was obtained using self-truncated ionization injection^[85]. The use of two-color ionization injections has enhanced the control over the accelerated beam^[86]. For high-energy acceleration, a novel approach to staged LWFA employing a curved plasma channel was theoretically proposed, and the essential processes of relativistic laser guiding and LWFA in a curved plasma channel were

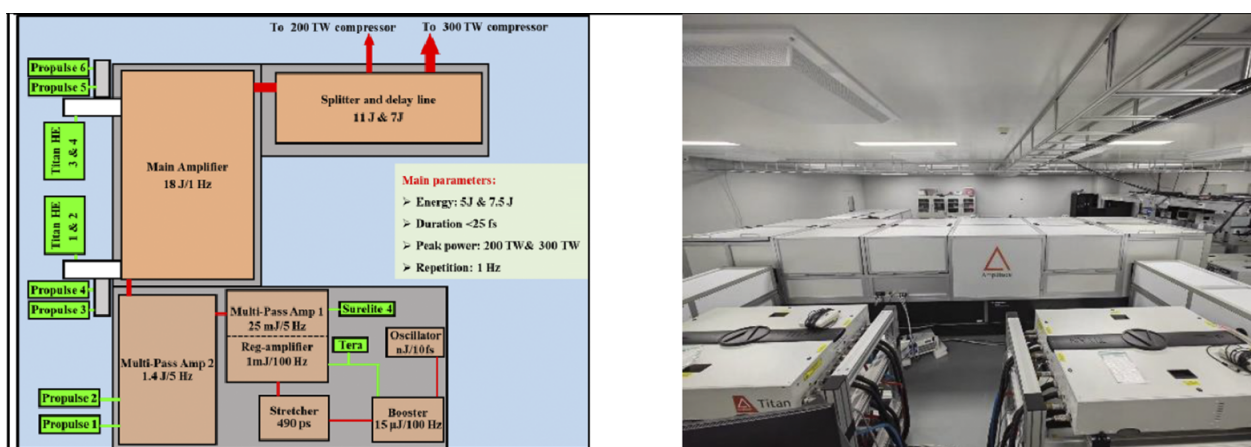


Figure 10. The 200 and 300 TW laser system.



Figure 11. The vacuum chambers in the experimental area.

experimentally validated^[88,89]. Regarding radiation sources, mJ-level THz radiation has been successfully generated from laser–solid target interactions through coherent transition radiation and from laser–gas interactions through mode conversion of the laser wakefield^[18,21,90]. A method to enhance harmonics generation from laser–solid interactions by modifying the surface-plasma profile was also proposed and verified. This modification not only enhances the radiation intensity but also broadens the spectral output^[91,92]. For applications, femtosecond laser-induced Coulomb excitation of ions, facilitated by quivering electrons, has been utilized to pump nuclear isomeric states^[93]. A novel method involving an ultra-high-current electron beam, accelerated by an intensely focused laser self-guiding in dense plasma, has been employed for pumping nuclear isomers^[94]. These advancements illustrate effective methods to rapidly excite nuclei using femtosecond lasers, which could profoundly impact research into nuclear transition mechanisms and the development of nuclear gamma-ray lasers.

In future studies, both fundamental and applied researches will concentrate on the capabilities of the CLEF. In the obtuse angle chamber, experiments involving collisions between laser wakefield accelerated GeV-level electrons and intense laser fields – characterized by special modes and normalized intensities approaching 10 – will be conducted. These experiments aim to explore quantum electrodynamics (QED) plasma-related physics, including radiation reaction, nonlinear Compton scattering, gamma-ray generation and positron production. In the acute angle chamber, applications related to plasma optics, such as plasma optical modulators, plasma focusing lenses, relativistic mid-infrared radiation sources and staged LWFA, will be performed. A third target chamber has been designated for terahertz generation, high-harmonic generation (HHG) and other flexible applications.

2.5.2. Tsung-Dao Lee Institute

The 2.5 PW laser facility is an integral component of the Laboratory Astrophysics Platform (LAP) at the TDLI, SJTU. The TDLI is committed to addressing foundational scientific challenges, advancing the frontier of knowledge in fields such as astronomy and astrophysics, particle and nuclear

physics and condensed matter physics. It aims to reveal the connections between macroscopic and microscopic phenomena in the universe and to unravel the fundamental laws of interaction within nature. The institute explores extreme natural conditions, artificially created extreme conditions and cutting-edge detection methods to explore and manipulate novel physical states. Within the LAP, the 2.5 PW laser facility has been instrumental in creating extreme conditions for studying laboratory astrophysics, nuclear physics and nuclear astrophysics.

The 2.5 PW laser at the TDLI LAP utilizes titanium-sapphire CPA technology. The initial laser pulse is generated by an ultra-wideband Ti:sapphire self-mode-locked oscillator, and this seed pulse is subsequently stretched to nearly 1 ns in duration using a pulse stretcher. The pulse undergoes extensive amplification through multiple stages, with the final pulse energy nearing 80 J. Finally, this pulse is compressed to a duration of 22 fs by a grating compressor, achieving a peak power that exceeds 2.5 PW, as illustrated in [Figure 12](#).

During the transmission amplification process, the laser pulse traverses numerous optical components – mirrors, lenses and crystals – where the wavefront of the beam becomes distorted due to the inhomogeneity of the optical elements and machining defects. To enhance the near-field quality of the beam, an AO system has been implemented for closed-loop correction of the wavefront following the final amplifier. Concurrently, an XPW unit has been integrated at the front-end of the laser facility to enhance the time-domain contrast of the output laser. In the near future, the incorporation of a PM between the pulse compressor and the target chamber is planned to further improve the laser contrast.

The primary research objective of the LAP is to generate ultra-intense particle beams or X/γ-ray radiation via the QED effect using a PW laser, and subsequently to investigate topics in relativistic laboratory astrophysics, including the mechanisms of cosmic energetic particle/ray acceleration and nucleosynthesis processes related to the Big Bang, stars and supernovae. The experimental setup of the LAP comprises a dual-arm output 2.5 PW Ti-sapphire laser and a series of vacuum experimental chambers, as illustrated in [Figure 13](#). The focused laser achieves a maximum intensity

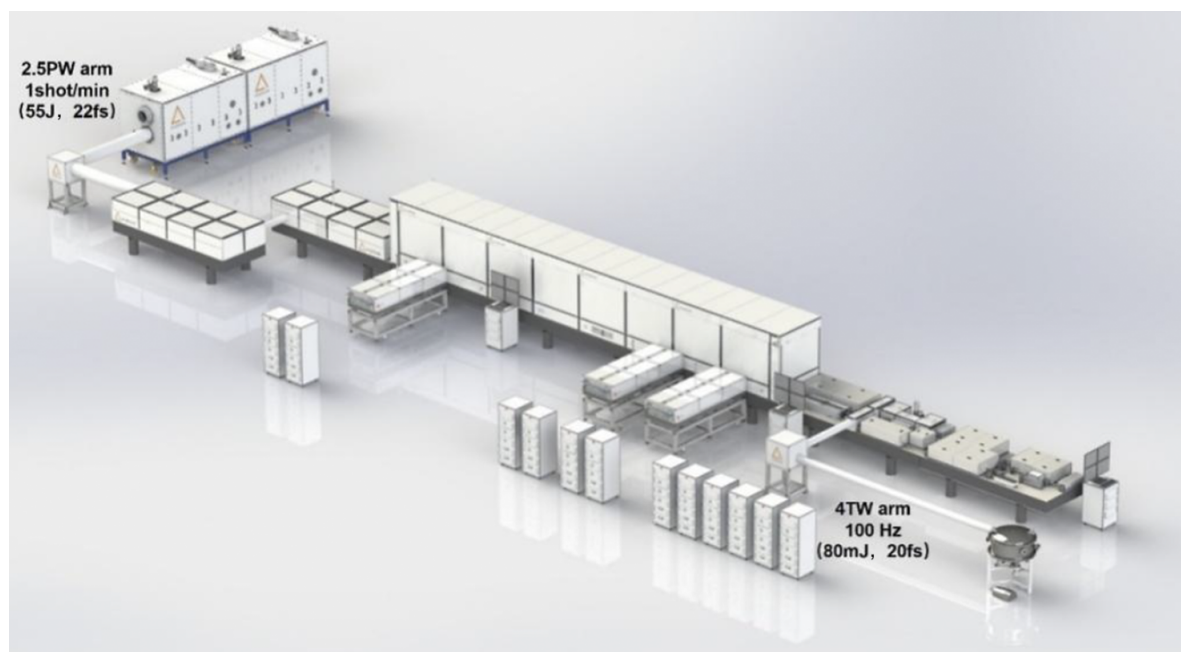


Figure 12. Diagram of the TDLI-LAP 2.5 PW laser.

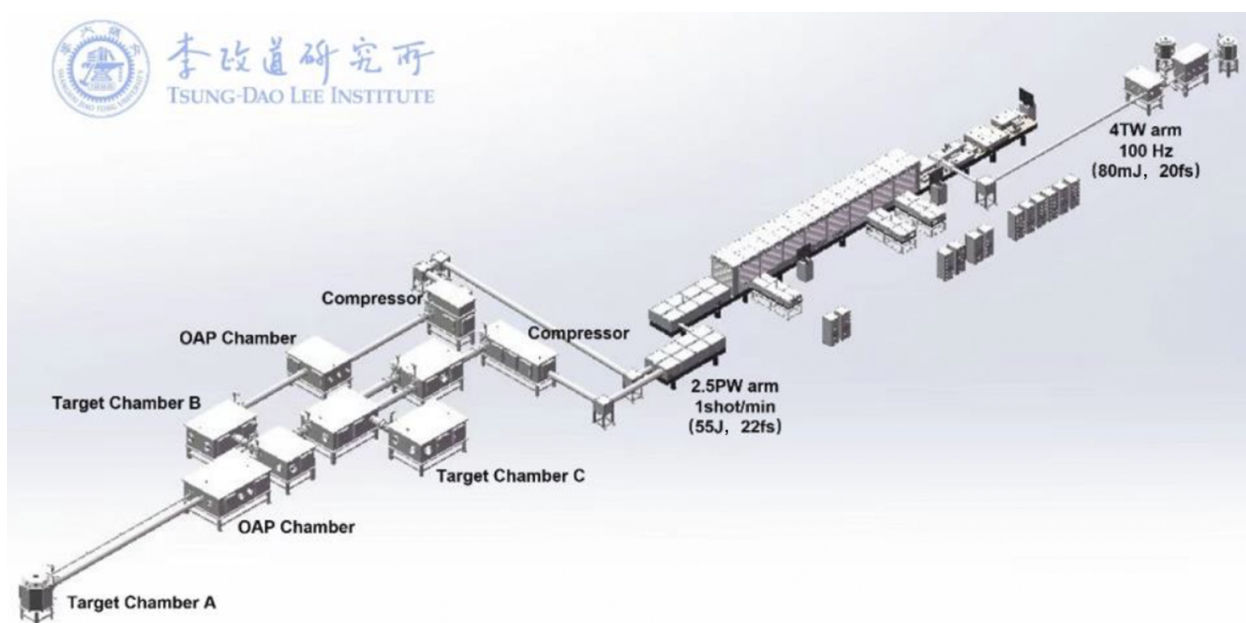


Figure 13. Design drawing of the LAP.

of 10^{23} W/cm², which is optimal for eliciting the QED effect in experiments. The main output laser, with a peak power of 2.5 PW and a repetition rate of one shot per minute, is equipped with three independent target chambers, described briefly as follows. (1) The long-focus laser target chamber is designed for LWFA to multi-GeV electron beams, facilitating the creation of ultra-dense and relativistic electron-positron plasmas for the study of relativistic astrophysical processes. (2) The short-focus laser target chamber aims to utilize maximum laser intensity to drive the QED

effect via nano-structured solid targets, generating an ultra-bright γ -ray source. This facility is pivotal for studying nuclear reactions under high-temperature and high-density conditions to simulate nucleosynthesis events such as the Big Bang and supernovae, and for conducting ultra-high-efficiency nuclear reactions for the precise measurement of nuclear data with high signal-to-noise ratios. (3) The laser beam collision target chamber focuses on exploring QED effects through a Thomson scattering scenario and the efficient generation of particle/radiation sources, including

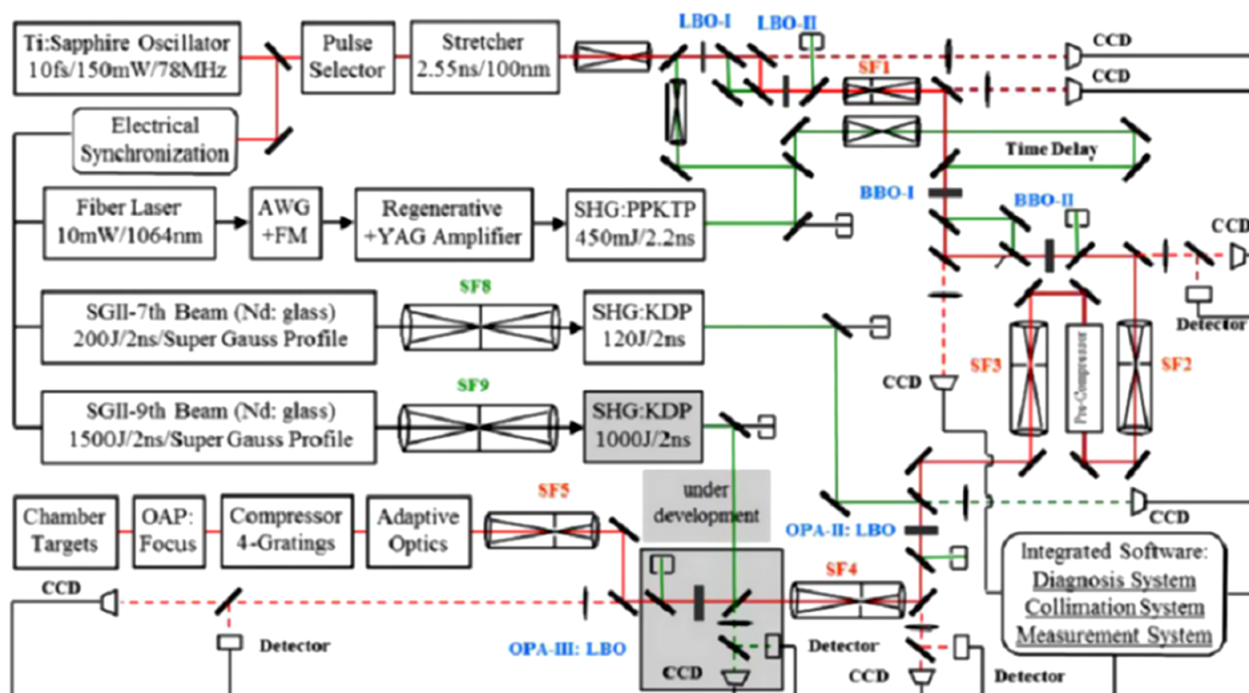


Figure 14. Schematic diagram of the SG-II 5 PW facility. OAPM, off-axis parabolic mirror; FM, frequency modulator; AWG, arbitrary waveform generator^[95].

the generation of γ -rays with orbital angular momentum. This chamber aims to investigate the structure of nuclei with yet undiscovered high-spin states or nuclear transition mechanisms.

For the minor stream, the laser system possesses a peak power of 4 TW and operates at a repetition rate of 100 Hz. This configuration is primarily utilized for applications that require high-repetition-rate electron, X-ray and neutron sources based on laser–plasma acceleration. The range of application tools includes, but is not limited to, advanced diagnostic techniques such as ultrafast X-ray imaging, X-ray absorption spectroscopy, X-ray diffraction and UED.

2.6. National Laboratory on High Power Laser and Physics, Shanghai Institute of Optics and Fine Mechanics

The SIOM National Laboratory on High Power Laser and Physics (NLHPLP) established a SG-II multi-functional experimental platform dedicated to the research and development of ICF and a broad range of high-energy-density physics^[95]. The platform consists of a SG-II laser facility, SG-II UP nanosecond and picosecond laser facility and SG-II femtosecond laser facility. The SG-II femtosecond laser facility and SG-II UP picosecond laser facility operated at the PW class scale.

2.6.1. SG-II femtosecond petawatt laser facility

The SG-II femtosecond petawatt laser facility, referred to as the SG-II 5 PW, employs a multi-stage noncollinear OPCA system based mainly on the SG-II nanosecond laser facility

as its high-quality pump source^[96]. The key technological advancements of the SG-II 5 PW include high-energy, high-efficiency OPCA, compensation for chromatic aberrations, spatiotemporal measurement and optimization and enhancements in pulse contrast through PMs. These improvements have substantially enhanced the performance of the laser output.

The SG-II 5 PW is engineered to deliver 150 J of laser energy with a pulse duration of 30 fs, centered at a wavelength of 808 nm. A schematic of this system is depicted in Figure 14. The initial chirped seed pulse from the stretcher is amplified through a three-stage OPCA process, utilizing frequency-doubled laser pulses from the SG-II laser facility as the pump source. The amplified laser pulse is then expanded to a 29 cm \times 29 cm aperture using multi-stage spatial filters. Its wavefront is meticulously measured and corrected via an AO system, ensuring exceptional beam quality. Subsequently, the pulse is directed into a four-grating compressor equipped with gold-coated gratings, where it is compressed into femtosecond pulses.

Currently, the final stage of the OPCA system remains under construction. The two-stage optical-parametric chirped-pulse amplifiers have achieved a spectral width of 85 nm and a chirped-pulse energy of 49.7 J. This output is compressed to a pulse duration of 21 fs (FWHM), as determined by an autocorrelator, achieving a compressor efficiency of 75%. The system is capable of delivering up to 1.76 PW of peak power with outstanding beam quality to the target chamber. The fundamental output parameters of the SG-II 5 PW are outlined in Table 3.

Table 3. Basic parameters of the SG-II femtosecond petawatt laser facility.

Facility	Spectral width (nm)	Pulse energy (J)	Pulse duration (fs)	Peak power (PW)	Focused intensity (W/cm ²)
SG-II femtosecond petawatt laser facility	85	37	21	1.76	10 ²⁰

Table 4. Basic parameters of the SG-II UP picosecond petawatt laser facility.

Facility	Pulse energy (J)	Pulse duration (ps)	Peak power (PW)	Focused intensity (W/cm ²)	Pulse contrast	Target aiming accuracy (μm)	Synchronization accuracy (ps)
SG-II UP picosecond petawatt laser facility	300–1000	0.7–10	1	10 ²⁰	10 ⁸	9.5	7.6

Research activities at the SG-II PW facility

A range of high-energy-density physics experiments have been conducted at the SG-II femtosecond petawatt laser facility, including investigations into laser proton acceleration, laser wakefield electron acceleration and ultrafast spatiotemporal physical dynamic diagnosis. Complementary experimental diagnostic techniques and target fabrication methods have also been developed to support these studies. To meet various experimental requirements, the SG-II 5 PW includes two target chambers and multiple operating modes.

Since its commissioning in 2017, the SG-II 5 PW laser has been focused using an $f/3$ OAP mirror in a short-focus target chamber. This configuration has proven effective in laser proton acceleration research, achieving a consistent proton energy of 16 MeV in 2019.

In 2020, a new operational mode was introduced where the femtosecond PW laser was synchronized with a 100-J nanosecond laser, allowing both to be fired simultaneously with high-precision timing and target aiming accuracy. The addition of the nanosecond pulse facilitated the achievement of a proton energy of 23.3 MeV.

Since 2021, a long-focus target chamber has been operational for research into laser wakefield electron acceleration. This chamber features a focal length of approximately 10 m, which provides a long Rayleigh length and a substantial acceleration volume. An auxiliary femtosecond probe pulse, synchronized with the main pulse, was introduced to dynamically diagnose the plasma density. The accelerated electron beam was then measured using an absolutely calibrated imaging plate and a dipole magnet.

2.6.2. SG-II UP laser facility

The SG-II UP laser facility includes eight 10-kJ-class nanosecond laser beamlines, collectively known as the SG-II UP nanosecond laser facility, and one kJ-class picosecond laser beamline, referred to as the SG-II UP picosecond petawatt laser facility, as depicted in Figure 15.

The SG-II UP nanosecond laser facility employs an innovative multi-pass amplification architecture featuring a large-aperture plasma electrode Pockels cell (PEPC). The primary amplification modules comprise a four-pass cavity amplifier and a two-pass power amplifier, both utilizing neodymium glass. Spatial filters and large-diameter

deformable mirrors are implemented to maintain high beam quality. At 1ω (1053 nm) wavelength, each beam can achieve a maximum energy output of 8.05 kJ over 5 ns, with a routine total energy output of 40 kJ in 3.3 ns. These amplified 1ω laser pulses are directed into the final optics assembly (FOA), where they are converted into 3ω (351 nm) ultraviolet (UV) laser pulses through frequency tripling and subsequently focused onto the target using a wedge lens. The maximum energy per 3ω pulse can reach 5 kJ over 4.6 ns, with a routine total 3ω energy of 25 kJ in 3.3 ns.

The SG-II UP picosecond petawatt laser facility integrates the technical advantages of OPCPA and CPA^[97]. This integration has led to several significant technological advancements, including broadband chirped-pulse amplification, large-aperture pulse compression and focusing and the ability to measure single-shot high-energy picosecond-pulse contrast. The initial seed pulse is stretched and subsequently amplified by a high-power OPCPA pre-amplifier, which provides substantial gain and a specific spectral structure^[98]. The main amplifier utilizes a neodymium glass CPA within a master oscillator power amplifier (MOPA) system, facilitating the achievement of high-energy output in the kJ range. Following amplification, the kJ-level laser pulse is compressed into a picosecond pulse using a large-diameter, four-grating compressor, resulting in an output of 1 kJ over 1.7 ps. The petawatt-class ultrashort pulse laser is focused using an OAP mirror to achieve an intensity of 10²⁰ W/cm² and a pulse contrast of 10⁸ (measured 82 ps before the main pulse). Furthermore, the SG-II UP picosecond petawatt laser facility boasts high-precision target aiming and excellent time synchronization capabilities with the SG-II UP nanosecond laser facility, featuring a target aiming accuracy of 9.5 μm (RMS) and a time-synchronization accuracy of 7.6 ps (RMS). Table 4 shows the main parameters of the SG-II UP picosecond petawatt laser facility.

Research activities at the SG-II UP facility

The SG-II UP facility is fully equipped to support a broad spectrum of experimental needs in laser physics, either independently or in conjunction with the SG-II UP nanosecond laser facility. It includes a comprehensive set of standard

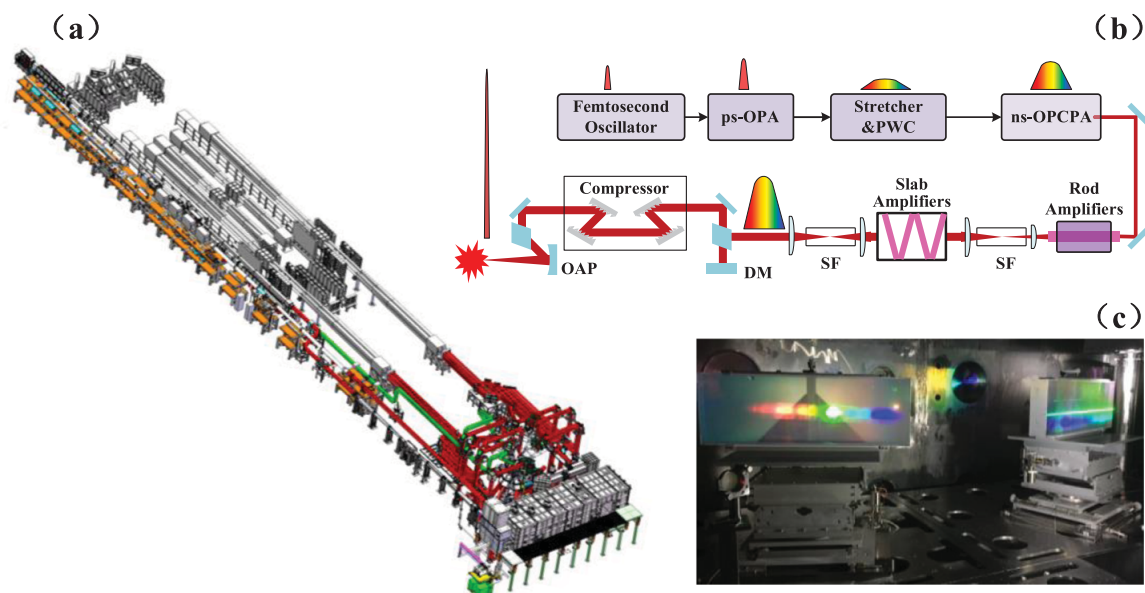


Figure 15. (a) Overview of the SG-II UP laser facility. (b) Schematic diagram of the SG-II UP picosecond petawatt laser facility. (c) Large-aperture grating pulse compressor.

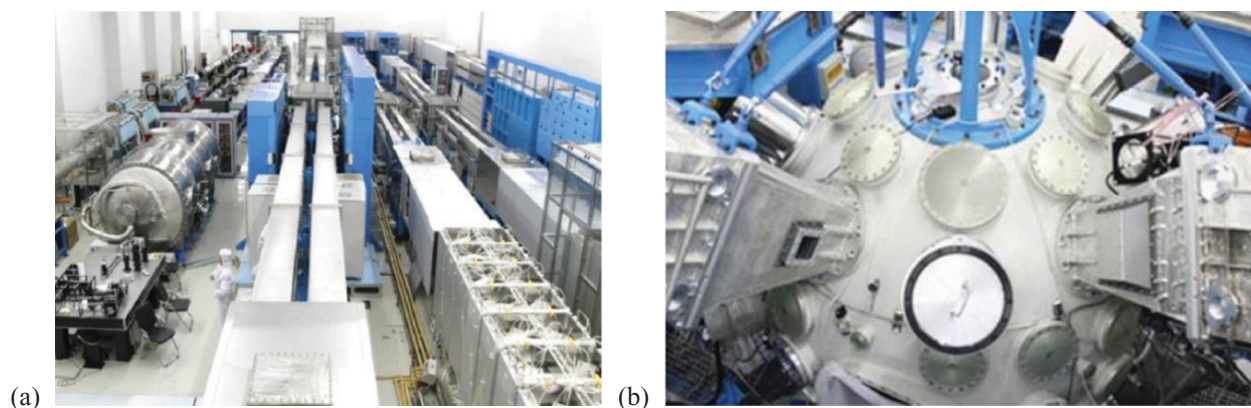


Figure 16. (a) Laser bay of the SG-II UP laser facility. (b) Target chamber of the SG-II UP laser facility^[94].

diagnostic instruments, such as spectrometers for X-ray, UV and visible light; streaked cameras for X-ray and visible light; a near-backscatter imager; and spectrometers designed to measure the energy of electrons, ions and protons. Figure 16 shows the laser bay and the target chamber of SG-II UP laser facility.

The SG-II UP picosecond petawatt laser facility has played a pivotal role in advancing laser proton acceleration experiments. In 2017, proton energies exceeding 50 MeV were measured using a Thomson spectrometer, and by 2021, proton beams with energies greater than 70 MeV had been achieved^[99]. The proton beam generated by the SG-II UP picosecond petawatt laser facility has been employed for proton radiography to investigate the kinetic effects in ICF physics.

In collaboration with the SG-II UP nanosecond laser facility, the picosecond petawatt laser facility has facilitated

research in FI, a highly promising method for achieving high gain in ICF. In 2020, the SG-II UP laser facility conducted the world's first experiment on indirect-drive FI^[100]. The observed neutron gain was greater than 44, successfully verifying the validity of fuel heating using the SG-II UP picosecond petawatt laser facility^[101].

In addition, the SG-II UP picosecond petawatt laser facility can be configured to operate in nanosecond pulse mode by modifying its seed pulse and terminal configuration, delivering a 3 kJ/3 ns/3 ω output. This capability serves as a probing beam for the SG-II nanosecond laser facility, offering versatility in adjusting the pulse width from tens of picoseconds to nanoseconds, with outputs available at various harmonic frequencies (1ω , 2ω , 3ω and 4ω).

In 2024, the SG-II UP laser facility is scheduled for a significant upgrade to include 16 nanosecond laser beamlines and 2 picosecond petawatt laser beamlines. This expansion

is expected to introduce additional joint operation modes, including the simultaneous use of two kJ-class picosecond petawatt lasers and a combination of these lasers with the 16-beam nanosecond lasers. These enhancements will substantially increase the capability of the laser facilities and expand the scope of experimental physics that can be explored.

2.7. State Key Laboratory of High-Field Laser Physics, SIOM/ShanghaiTech University

In 2007, the team from SIOM State Key Laboratory of High-Field Laser Physics (LHFLP) successfully developed a high-intensity (0.89 PW/29.0 fs) femtosecond laser system^[102]. In 2013, they developed technologies such as parasitic oscillation suppression, precise spatiotemporal control, high-gain Ti:sapphire amplification and ultra-high temporal contrast, and successfully developed a 2.0 PW laser^[103]. In 2014, based on a 150 mm Ti:sapphire crystal, they further obtained an amplified output of 192.3 J and a compressed pulse width of 27.0 fs, corresponding to a peak power of 5.13 PW^[104]. At that time, these lasers had the highest peak powers worldwide. In recent years, several ultra-intense and ultrafast laser facilities have been developed. The progress in the development of these three facilities is discussed below.

In 2012, a 200-TW laser was constructed under the National Major Scientific Research Instrument Development Project, funded by the National Natural Science Foundation of China. By 2015, SIOM had completed and commissioned a 200 TW/1 Hz Ti:sapphire laser, which has since been utilized for applications in LWFA, HHG and X-ray free electron laser (XFEL) projects. In 2018, the team optimized the laser design and constructed a new 200 TW/1 Hz Ti:sapphire laser setup to enhance the LWFA performance and advance the XFEL project. Figure 17(a) illustrates a diagram of the new setup, which includes a Ti:sapphire oscillator, Offner stretcher, regenerative amplifier, multi-pass amplifier, power amplifier, final amplifier, six Nd:YAG lasers and a vacuum compressor. The optimized laser is capable of generating a 200-TW-level peak power without a full pump load, ensuring stable long-term operation. An energy attenuation module was also installed between the final amplifier and the vacuum compressor. This module characterizes various laser parameters under full-energy amplification conditions, such as the compressed pulse duration, focal spot size and beam pointing on the target, while reducing the laser energy to manageable levels without altering the pulse properties. The output parameters of each laser module are detailed in Figure 17(a), and a schematic of the setup is shown in Figure 17(b).

The enhanced 200 TW/1 Hz Ti:sapphire laser has significantly advanced LWFA experiments. In these experiments, electron beams were produced using density downramp injection within the blowout regime. The system utilized a 0.8 mm thick gas jet containing pure helium at a plasma

density of $(5 \pm 0.5) \times 10^{18} \text{ cm}^{-3}$. These electron beams were deflected by a 1.1 T magnet and detected by a Lanex phosphor screen, and subsequently imaged by an intensified charge-coupled device (CCD) camera in single-shot mode. For accurate charge measurements, the camera was calibrated against a calibrated imaging plate and an integrating current transformer. The stability of the driving laser has significantly enhanced the reproducibility of the electron beams in the LWFA experiments. Under optimal conditions, quasi-monoenergetic electron beams were consistently produced, achieving nearly 100% reproducibility over 300 consecutive shots, with an average peak energy of approximately 667 MeV and a standard deviation of 3.4%. This represents a major improvement from earlier experiments, which only achieved 30% reproducibility and experienced a 10% fluctuation in peak energy. The energy spectra of the first 20 consecutive electron beams are shown in the insets. In addition, these electron beams generate X-ray radiation after passing through undulators, marking a significant development in compact XFELs^[106].

In 2016, the Shanghai Super-intense Ultra-fast Laser Facility (SULF) project, supported by the Chinese and Shanghai local governments, was approved and ultimately completed at the Zhangjiang location by the end of 2020. The SULF contains three laser beamlines and three user platforms.

The setup at SULF includes three beamlines: a 10 PW laser firing at a rate of one shot per minute, a 1 PW laser operating at 0.1 Hz and a 100 TW laser running at 1 Hz. Each beamline is equipped with its own pulse compressor, enhancing their operational flexibility. Both the 10 and 1 PW lasers utilize the same oscillator and are powered through two parallel amplification paths. The 100 TW laser is derived from a beam splitter placed at the output of the 1 Hz pre-amplifiers used for the 10 PW laser. This arrangement allows each beamline to be used either independently or in combination, supporting a wide variety of experimental applications. Figure 18 shows the layout of the SULF facility.

The core component of the SULF is its 10 PW laser system. In early 2016, a prototype of the SULF was developed in a nearby building to conduct preliminary research and assess the performance of its subsystems. By the end of 2016, this prototype achieved an output of 5.4 PW^[107] and, in 2017, demonstrated 339 J energy output using 235-mm-diameter Ti:sapphire CPA^[108]. The construction of the SULF building was completed in June 2018, after which the laser systems were relocated and reinstalled to establish the SULF as a user facility. Leveraging the insights gained from the prototype, several subsystems were redesigned and the entire 10 PW laser system was upgraded. A key enhancement at the SULF-10 PW facility was the implementation of temporal contrast enhancement using a dual CPA strategy^[109,110]. Initially, a Ti:sapphire laser with a 6 mJ pulse energy operating at a 1 kHz repetition rate served as the primary CPA stage. A pulse cleaner, based on cross-polarized wave generation

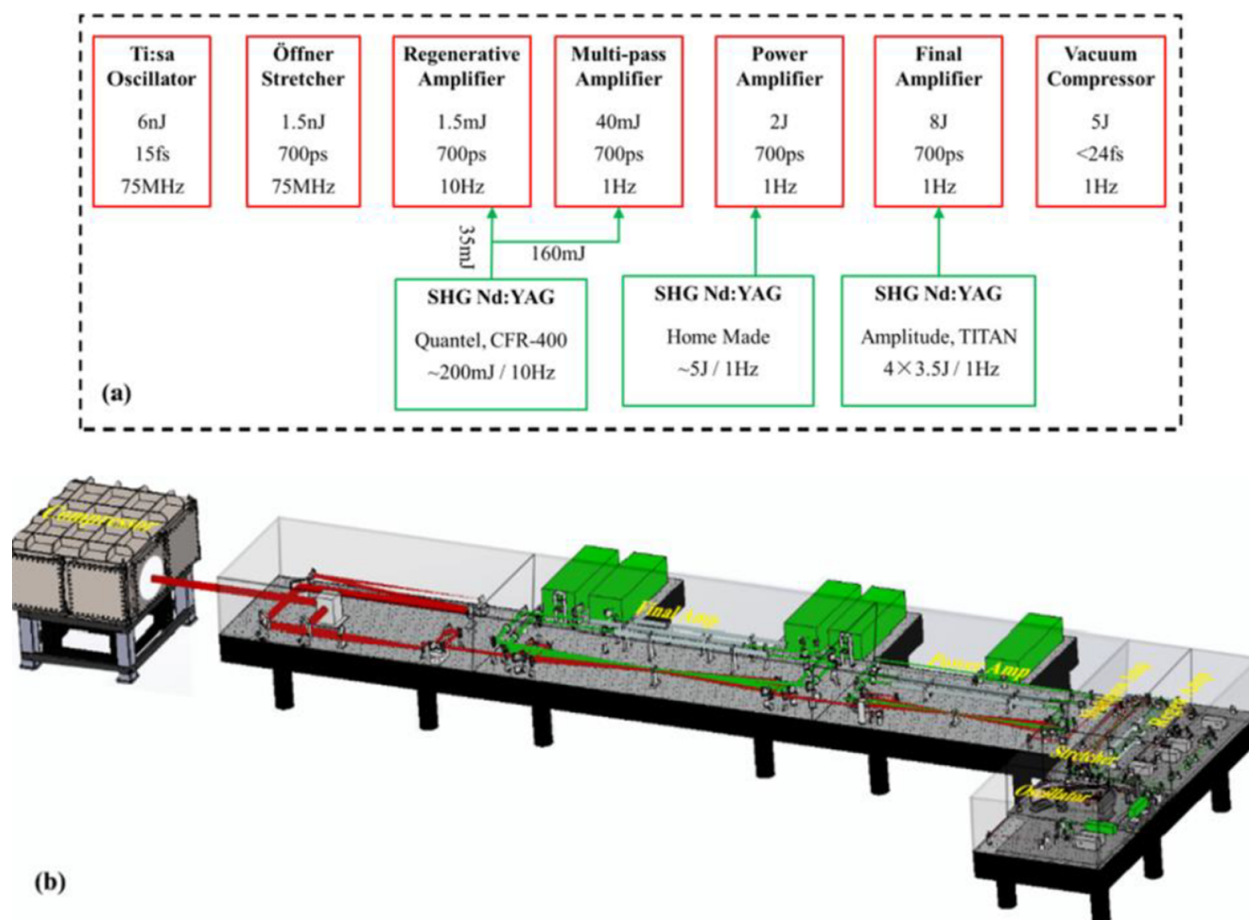


Figure 17. Layout (a) and schematic drawing (b) of the 200 TW/1 Hz Ti:sapphire laser^[105].

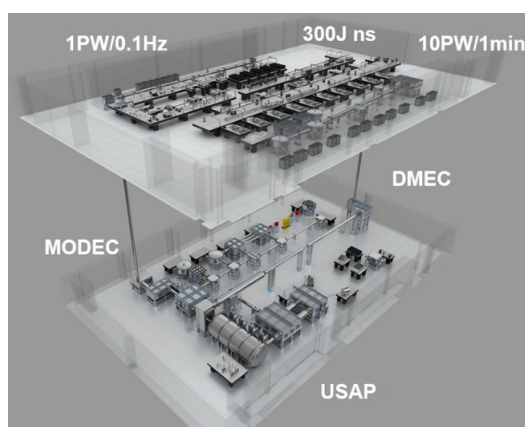


Figure 18. Layout of the SULF.

(XPWG) and optical-parametric amplification (OPA), was employed to produce a high temporal contrast seed pulse with 100 μJ energy and a contrast ratio of 10^{12} . This setup was followed by five stages of Ti:sapphire amplification, boosting the pulse energy to approximately 400 J. The 10 PW compressor was constructed using four large gold-coated gratings (575 mm \times 1015 mm), supplied by Horiba JY^[111].

A Wizzler–Dazzler feedback loop system was integrated for dispersion management and optimization of the compressed pulse duration. The duration of the compressed pulse was measured to be 2.4 fs. The overall transport efficiencies of the large-aperture periscope, achromatic image relay system and grating compressor were quantified at 70.52%. The peak power of the final compressed femtosecond laser pulse was calculated to be 12.8 PW, derived by dividing the pulse energy by the compressed pulse width. The setup of the SULF 10 PW laser system is depicted in Figure 19.

The SULF-1 PW laser beamline employs a dual CPA configuration, achieving laser pulses with an energy of 50.8 J at a 0.1 Hz repetition rate following the final amplification stage (see Figure 20). This setup exhibits remarkably low shot-to-shot energy fluctuations, recorded at just 1.2% (standard deviation)^[112]. Upon compression, the pulse duration is reduced to 29.6 fs, achieving a maximum peak power of 1 PW. The contrast ratio at 80 ps prior to the main pulse reaches 2.5×10^{11} . Optimization of the angular dispersion within the grating compressor has refined the focused peak intensity. Measurements over a period of 1 hour show horizontal and vertical angular pointing fluctuations of 1.89 and 2.45 μrad (std), respectively. The moderate repetition



Figure 19. Picture of the SULF-10 PW system.

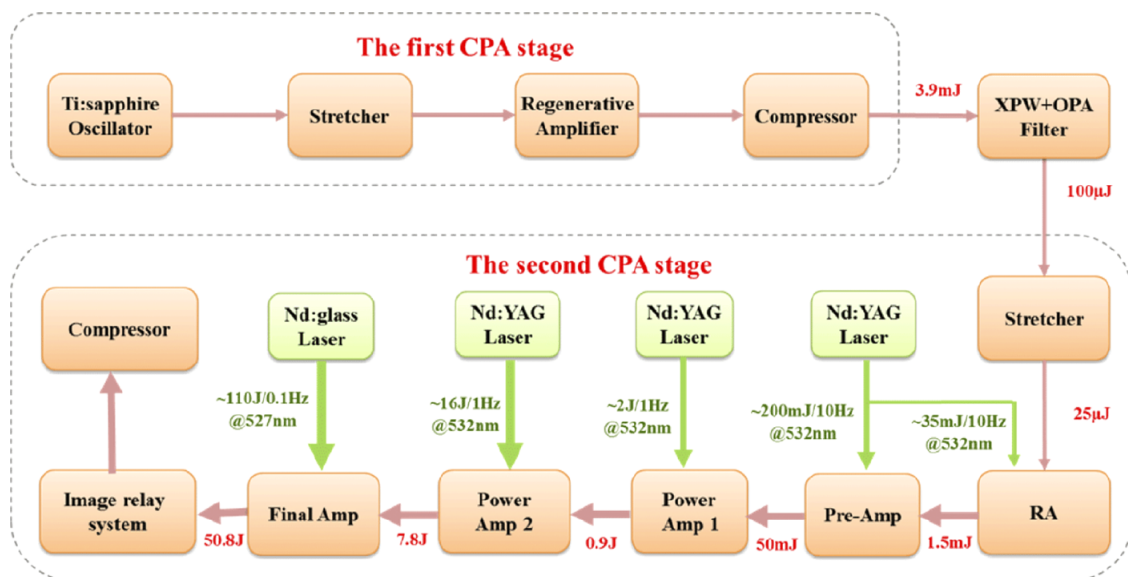


Figure 20. Framework diagram of the SULF-1 PW beamline.

rate and consistent stability of the beamline are particularly advantageous for studies involving laser–matter interactions. Currently in the commissioning phase, the SULF-1 PW laser beamline is conducting preliminary experiments on particle acceleration and secondary radiation at 300–400 TW/0.1 Hz laser conditions. The progress in these experimental endeavors and the consistent operational performance of the laser have affirmed the reliability of the SULF-1 PW beamline.

The outputs from the laser system, along with the secondary radiation and particle sources generated, serve diverse scientific purposes across three distinct experimental end stations.

(1) DMEC (dynamics of materials under extreme conditions) end station. The DMEC end station has been designed to facilitate a range of inquiries, including high-order harmonic generation via intense ultrafast laser pulses, characterizing the dynamics of critical

materials under extreme conditions and performing nondestructive evaluations of both aerial and nuclear materials^[113].

(2) USAP (ultrafast subatomic physics) end station. The USAP end station has been customized to support investigations into a variety of phenomena, such as the acceleration of charged particles (both electrons and protons) to relativistic speeds, the exploration of extreme phenomena within strong-field QED and studies in photonuclear physics^[114].

(3) MODEC (molecular dynamics and extreme-fast chemistry) end station. The MODEC end station has been engineered to accommodate diverse research objectives, including the detection and manipulation of chemical reactions, exploration of the structures, dynamics and interactions of macromolecules and generation of intense terahertz radiation^[115].

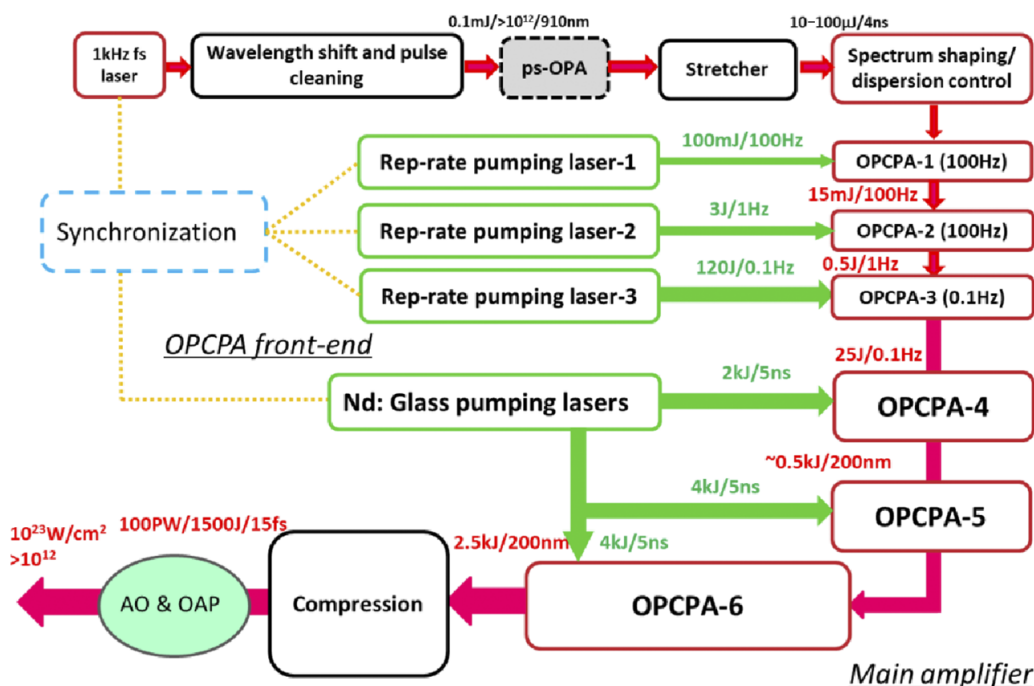


Figure 21. Schematic diagram of the SEL-100 PW laser.

In 2018, the Station of Extreme Light (SEL) project, supported by both the Chinese and Shanghai local governments, was approved. It is currently under construction at Zhangjiang and serves as an end station of the Shanghai high-repetition-rate XFEL and Shanghai high-repetition-rate XFEL and extreme-light facility (SHINE). The core component of the SEL project is a 100 PW laser system, which is engineered to achieve a focused intensity of 10^{23} W/cm^2 ^[116].

The SEL-100 PW utilizes OPCPA technology, which is pivotal due to its minimal thermal impact, broad gain bandwidth and compatibility with large-aperture devices, driving advancements in 100-PW laser systems. The SEL-100 PW is designed to deliver 1.5 kJ of energy within a 15 fs pulse duration. Constructing such formidable laser systems demands large-aperture nonlinear crystals that can endure energies exceeding 10 kJ. Among these, the deuterated potassium dihydrogen phosphate (DKDP) crystal is particularly notable due to its capability to grow to sizes larger than 400 mm and its use in ICF laser facilities. Consequently, adopting DKDP-based OPCPA presents a promising approach for developing 100-PW femtosecond lasers.

Figure 21 depicts the conceptual design of the SEL-100 PW laser system, which incorporates an all-OPCPA architecture. This system integrates an ultra-broadband seed, five nonlinear optical-parametric amplification (NOPA) stages each with their respective pump lasers, a stretcher, a compressor and synchronization apparatus. Maintaining a bandwidth exceeding 200 nm is crucial for achieving the 15 fs pulse duration. The front-end of the system is capable of delivering 25 J/0.1 Hz laser pulses with a chirped-pulse

duration of approximately 4 ns^[117,118]. At the core of the main amplifier, two-stage DKDP-based OPCPA systems are pumped with energies of 2 and 10 kJ in type-I phase matching. The 10-kJ pump laser emulates a NIF beam-line, boasting specifications of 10 kJ at 527 nm over 5 ns. The DKDP crystals used in the main amplifier have a deuteride rate of approximately 85%, with dimensions of 170 mm × 170 mm and 400 mm × 400 mm, and a thickness of 35 mm. Notably, all image relay telescopes within the main amplifier use all-reflective components to maintain an achromatic ultra-broadband laser beam. The target output for the 100 PW laser is 1500 J per pulse with a pulse duration of 15 fs. Given the damage threshold of the gratings, it is necessary to expand the beam size to 800 mm × 800 mm prior to compression to mitigate potential damage to the gratings within the compression chamber caused by the high peak power/intensity^[119]. The current grating size falls short of directly supporting the compression of a 100 PW (1.5 kJ/15 fs) laser, prompting ongoing research and development of a custom grating measuring 1.06 m × 1.6 m.

In 2021, a prototype of the SEL-100 PW front-end, based on three-stage OPCPA using a lithium triborate (LBO) crystal, was developed. This front-end, designed to be installed in the 100 PW laser facility, supports a spectral width exceeding 200 nm, a compressed pulse duration of 13.4 fs and a potential peak power exceeding 250 TW at a repetition rate of 0.1 Hz. The completion of the SEL-100 PW facility is anticipated by 2027.

The SEL facility represents a pioneering collaboration that combines a 100 PW optical laser with a hard XFEL, setting

the stage for advanced research in QED and other high-energy-density physics domains. This unique combination of capabilities is expected to usher in a new era of scientific exploration^[120].

Focusing the 100 PW laser to achieve intensities surpassing 10^{23} W/cm² on a target could create QED characteristic plasmas, potentially marking a significant milestone in scientific exploration. An XFEL beam, in tandem with the 100 PW laser, provides an ideal tool to probe these elusive phenomena. The emerging physics from this QED regime of laser–plasma interactions includes the efficient emission of gamma photons, the radiation-reaction effect and the QED cascade. By combining the world's most potent light sources, which emit at wavelengths of approximately 0.1 nm and approximately 1 μ m, researchers can explore a regime where the strong QED nature of the vacuum can be explored for the first time. The introduction of the SEL-100 PW laser also heralds a new era in high-field physics, offering revolutionary insights into light–matter interactions. The unprecedented light intensity of 10^{23} W/cm² will propel interactions into a strong relativistic regime, potentially enabling the acceleration of charged particles to unprecedented levels ranging from GeV to 100 GeV. Moreover, high-power lasers are capable of recreating exotic physical conditions akin to those found in the outer reaches of the universe, thereby facilitating the study of numerous astrophysical phenomena in laboratory settings, such as MR and the generation of extremely strong magnetic fields.

2.8. Shenzhen Technology University

The SZTU team has initiated the construction of a comprehensive ultra-intense laser platform that includes several ultra-intense laser facilities, integrated with a linear electron accelerator, dynamic high-pressure loading platforms and diamond anvil cells. This multifaceted platform will facilitate research in high-energy-density physics, the development of novel coherent light sources and the exploration of material properties under extreme high-pressure and high-temperature conditions.

Currently, a 200 TW laser system is under construction. This system is designed to deliver a 5 J laser pulse over a duration of 25 fs, achieving a peak power of 200 TW. It features a contrast ratio exceeding 10^{10} , and will primarily be used for experiments focused on laser–plasma interactions, particularly those involving the applications of laser-driven particles and radiation.

In addition, a kHz-TW laser system and its corresponding experimental beamline have been successfully installed. Featuring an OPCPA front-end in conjunction with several multi-pass amplifiers, this system generates outputs of 1 kHz/20 mJ/20 fs and 50 Hz/150 mJ/25 fs. The central wavelength of the Ti:sapphire-based laser is approximately

800 nm, and the pulse temporal contrast approaches 10^{10} . Thanks to the OPCPA front-end, a dedicated system design and an effective self-feedback mechanism, the kHz arm of the system is carrier-envelope phase (CEP) stabilized, ensuring a stability of less than 250 mrad over 10 shots and less than 300 mrad from shot to shot. A post-compression module featuring a 6-m-long hollow-core fiber is currently being assembled, which has enhanced the kHz arm to 12 mJ/3 fs. When combined with a tight focusing scheme, this few-cycle pulse achieves a peak intensity of 10^{20} W/cm² at kHz repetition rates. The enhanced capabilities of this upgraded system provide an exceptional experimental platform for studying plasma physics in the relativistic regime and for developing secondary sources, particularly coherent extreme ultraviolet (XUV) light sources through gas and surface-plasma HHG.

Research activities of the SZTU team

The SZTU team has been intensively engaged in advancing research in laser-driven particle acceleration, novel radiation sources, HHG and laser-driven nuclear physics. Recently, the team has spearheaded several groundbreaking studies focusing on the control of generation and transport processes of laser-driven high-current electron beams, as well as the development and metrology of coherent XUV sources.

In their efforts to generate highly charged electron beams, which are crucial for a wide range of applications, the team explored interactions between NCD plasma and lasers. Through these interactions, they successfully obtained a high-charge electron beam and conducted simulation studies on reducing the divergence angle through density modulation. They observed a bubble-like structure in the plasma, formed by reinjected electrons, which not only facilitated the acceleration of electrons but also helped preserve transverse emittance. This innovative approach led to the achievement of electron beams with more than 200 pC of charge, peak energies of 500 MeV and a divergence of less than 20 mrad. Moreover, this bubble-like structure also significantly enhanced the yield and energy of gamma photons, elevating them to MeV level^[121,122]. These results were verified using a 200 TW laser system.

Furthermore, transport of high-current relativistic electron beams (REBs) in plasmas represents a fundamental issue in high-energy-density spaces and laboratory plasma physics. The team focused on the microscopic transport of REBs within plasmas and uncovered several new results. These include the nanoscale electrostatic modulation of REBs in solid-density plasmas^[123] and the branching and stopping of REBs in porous materials^[124,125]. Based on these new phenomena, they further extended the applications of REBs to include generating coherent radiation sources, highly brilliant incoherent gamma rays and laser-driven nuclear physics. In particular, they proposed a new approach for producing coherent intense subcycle pulses by simply directing

an REB into a plasma with a density up-ramp^[126]. These findings are poised to captivate researchers across multiple disciplines.

In the metrology of coherent XUV sources, the team has recently demonstrated a high numerical aperture (NA ~ 0.15) Hartmann wavefront sensor, effective in the 10–50 nm spectral range with a detection accuracy of $\lambda/40$ at 32 nm^[127]. This sensor has been used in extreme ultraviolet (EUV) microscopy^[128] for free electron laser beams at FLASH-II, DESY, and has recently achieved a focal spot size below 100 nm at a wavelength of 13.5 nm using Schwarzschild optics. The team also developed code for the wavefront investigation of surface-plasma HHG in the far field^[129], which provides insight into the surface-plasma features by a retro-propagation process. Further experiments and simulations are underway with this research team based on the high-NA wavefront sensor and exclusive numerical code. Moreover, a spatially resolved temporal characterization scheme for plasma-based attosecond light sources was proposed using a detailed experimental design^[130]. This full-optical setup and single-shot measurement approach can also be extended to gas HHG-based attosecond pulses. With a full wavefront and temporal study of the surface-plasma HHG attosecond light source, the spatial, spectral and temporal phases can be accurately obtained experimentally, leading to an extensive understanding of the intense laser field and the induced XUV field. The high repetition rate and diverse optical options enable extensive spatial and temporal studies of attosecond light sources using the kHz-TW laser, further exploring the properties of relativistic plasmas.

2.9. National University of Defense Technology

The extreme condition physics group at the NUDT investigates fundamental and advanced challenges in atomic and molecular physics under extreme conditions such as high temperatures, pressures and densities, and strong fields. Furthermore, they also actively pursue interdisciplinary research in high-energy-density physics. Since 2006, this group has conducted research in strong-field ultrafast physics. In 2009, a laboratory using femtosecond laser systems capable of producing millijoule-level energy per pulse was established. They have achieved significant results in several areas, including terahertz pulse generation^[131], terahertz pulse diagnostics^[132], attosecond pulse production^[133] and ultrafast dynamics in atoms and molecules^[134–136]. They have also developed advanced theoretical models, such as quantum molecular dynamics^[137] and machine learning algorithms^[138,139], to simulate laser–matter interactions directly. The establishment of Hunan Key Laboratory of Extreme Matter and Applications in 2023 marks a recent milestone in this field. In future studies, the group plans to integrate strong-field ultrafast physics with high-energy-density physics, develop multispectral ultrafast

optical diagnostic techniques and apply these techniques to investigate the states, properties and dynamics of matter under extreme conditions.

The group is developing an advanced high-intensity laser system that synchronizes high-contrast 6 J, 30 fs, 5 Hz high-energy pulses with 26 mJ, 30 fs, 1 kHz high-repetition-rate pulses by locking the repetition frequencies of two independent oscillators. [Figure 22](#) shows a picture of the 200 TW laser system. The high-energy pulses are used to create extreme conditions and generate high-flux broadband light sources, while the high-repetition-rate pulses provide high-quality, low-jitter probing light sources. These unique output parameters give the system broad application prospects in cutting-edge research fields such as strong-field terahertz, high-brightness X-rays, high-flux isolated attosecond pulse generation and ultrafast diagnostics of warm dense matter. The laser system is currently in the commissioning stage and is expected to become operational in the latter half of 2024.

For strong-field terahertz and X-ray generation, the facility produces intense terahertz and X-ray radiation through laser–matter interactions, enabling research on high-flux and high-energy radiation generation at high repetition rates with high-precision detection. Applications include materials science, biomedicine, environmental monitoring and other research domains.

In attosecond pulse generation, a 200 TW laser is used to drive a long gas target, producing high-flux isolated attosecond pulses. The team is also developing single-shot attosecond pulse characterization techniques based on angular-resolved photoelectron spectroscopy and precise dispersion compensation schemes. Using attosecond transient spectroscopy, the dynamics of complex systems under extreme conditions are investigated, and attosecond photoelectron spectroscopy techniques are used for preliminary exploration of nonlinear attosecond physics.

Regarding the ultrafast diagnostics of warm dense matter, the group developed a system specifically designed for nonequilibrium transient diagnostics driven by a 200 TW high-energy pump laser. High-temperature plasma was generated using a frequency-doubled laser and gold film, and terahertz pulses were produced using a lithium niobate crystal. By employing a stair mirror instead of a flat mirror for single-shot detection, the group obtained terahertz time-domain conductivity data for gold in a warm dense matter state, providing experimental evidence for improving the theoretical models of high-energy-density materials.

2.10. Laser Fusion Research Center of China Academy of Engineering Physics

In 2000, the team at the Laser Fusion Research Center (LFRC), China Academy of Engineering Physics (CAEP) initiated the development of a Ti:sapphire femtosecond laser facility, designated as SILEX-I (superintense laser for exper-



Figure 22. The 200 TW laser system at the NUDT.

iments on extremes)^[140]. This laser system comprised three stages, delivering outputs of 5, 30 and 300 TW, with a maximum peak power of 286 TW achieved in 2004.

In 2009, the team began constructing the Xingguang-III (XG-III) laser facility, the first to output three beams with different pulse widths and wavelengths. By the end of 2013, this facility was completed, producing femtosecond, picosecond and nanosecond beams at wavelengths of 800, 1053 and 527 nm, respectively^[141] (see Figure 23). The femtosecond beam was upgraded using a SILEX-I laser^[139]. The upgraded system incorporated two CPA systems and a pulse filter based on XPW generation to improve the temporal contrast^[142]; the output energy was also significantly enhanced. The picosecond beam utilizes an OPA + Nd:glass mixed-amplification scheme. The seed pulse of the picosecond beam is generated from part of the output pulse of the femtosecond beam's pre-amplifier by supercontinuum generation and fs-OPA. This method ensures precise synchronization of the two beams since they originate from the same source. The signal pulse is further amplified using nanosecond OPA, a Nd:glass rod and a disk amplifier. The nanosecond beam shares the same front-end and pre-amplifier as the other beams. After amplification in the Nd:glass disk amplifier, the nanosecond beam is transmitted to the target area, and its frequency is doubled. A separate seed source is also provided for the nanosecond beam to allow for a larger time delay between it and the other two beams in some experiments. The output energies and pulse widths of the three beams were 20.1 J/26.8 fs, 370.2 J/0.48 ps (the shortest) and 575.4 J/1.0 ns, respectively^[140]. The shortest measured synchronization time (peak-to-valley) and shot-to-shot timing jitter were less than 1.32 ps. Characteristics such as precise synchronization and versatile multi-functional

laser beams make the XG-III laser facility a unique platform for pump-probe experiments, greatly enhancing the scope of physics experiments.

In 2013, the CAEP group initiated the construction of the SILEX-II laser facility, a fully integrated OPCPA system designed to achieve multi-petawatt peak laser power. As shown in Figure 24, the facility comprises a femtosecond oscillator, a ps-OPA front-end, an Offner stretcher, an ns-OPA pre-amplifier, an ns-OPA main amplifier and a compressor. The femtosecond oscillator provided an initial 10 fs, 800 nm pulse, which was stretched to 5 ps by an SF10 glass. The pulse energy was then amplified from 0.5 nJ to 2 mJ by the ps-OPA front-end, using a 10 mm × 10 mm × 10 mm beta barium borate (BBO) crystal. Subsequently, the pulse was stretched to 3 ns and amplified to 200 mJ using pre-amplifiers with a 15 mm × 15 mm × 15 mm LBO crystal. In the main amplifier, two LBO crystals, sized 165 mm × 120 mm × 10 mm and 130 mm × 130 mm × 10 mm, were used to achieve an output signal energy exceeding 150 J. Finally, the nanosecond pulse was compressed to approximately 20 fs using four large-scale gold-plated 1740 grooves/mm gratings (370 mm × 970 mm). In 2017, SILEX-II reported a compressed energy of 91.1 J and a pulse duration (FWHM) of 18.6 fs, resulting in a peak laser power of 4.9 PW.

Currently, updates to SILEX-II are focused on enhancing its stability. Compared to the previous version, an active pump-signal synchronization system has been employed at the front-end, reducing the RMS instability of the output energy from 30.3% to 3.15%. In addition, both the pre-amplifier and main amplifier have been upgraded from a single-stage to a dual-stage configuration to further improve the energy stability. In recent experiments, 15 shots achieved an average on-target energy of 61 J, demonstrating a stable capacity of 3 PW for physical experiments.

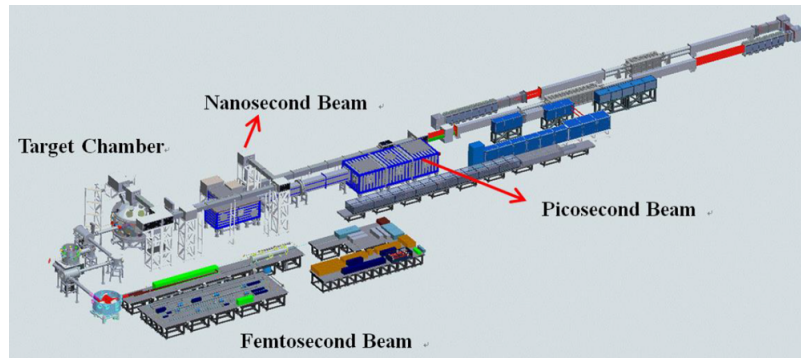


Figure 23. Layout of the Xingguang-III laser facility.

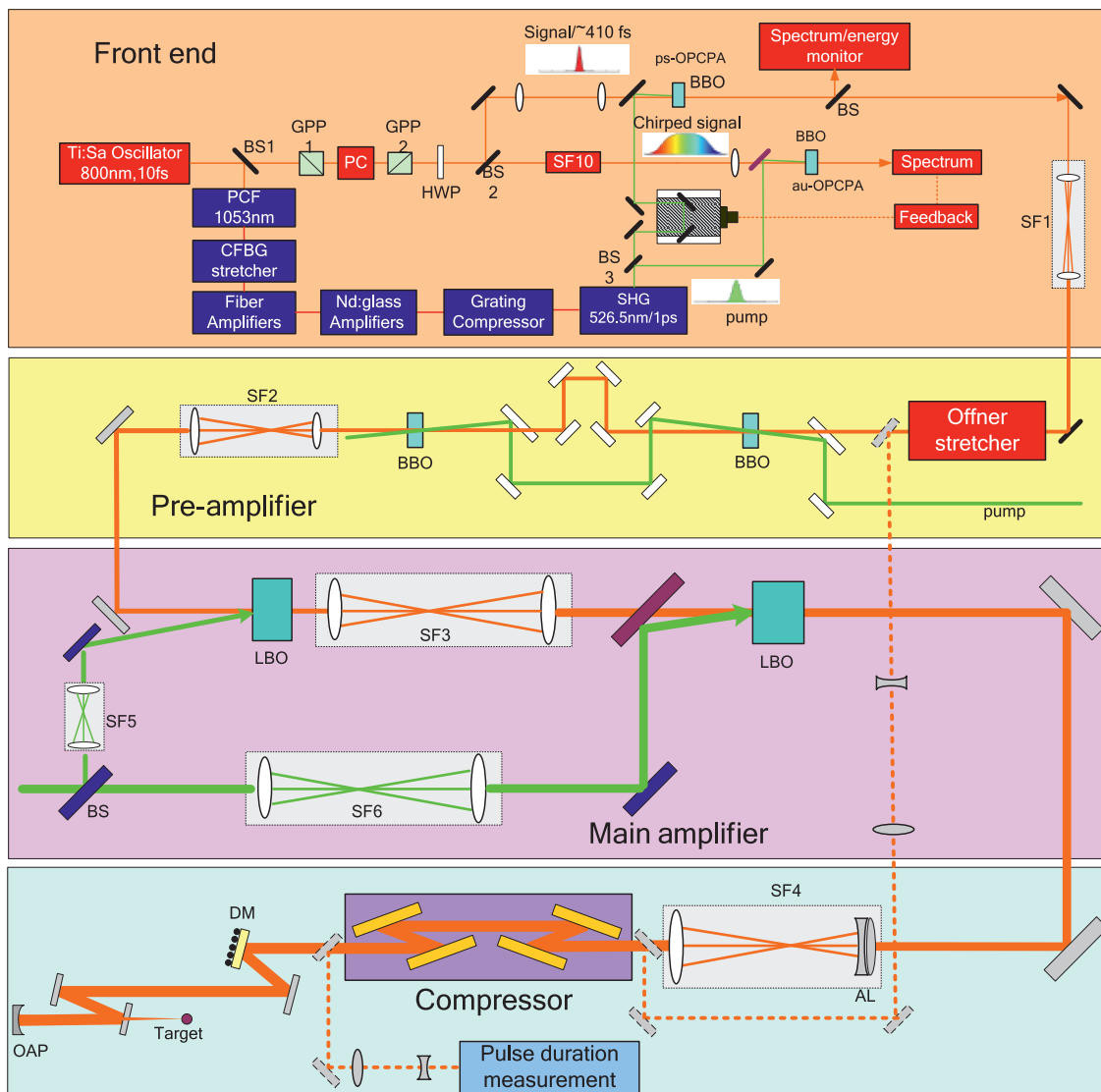


Figure 24. Schematic of the present SILEX-II whole-OPCPA laser system. PCF, photonic crystal fiber; CFBG, chirped fiber Bragg grating; BS, beam splitter; PC, Pockels cell; GPP, Glan prism polarizer; HWP, half-wave plate; SF, spatial filter; AL, achromatic lens; DM, deformable mirror; OAP, on-axis parabolic mirror.

Research activities of the LFRC team

The LFRC group focuses on the generation and application of radiation sources, including X-rays and protons, leveraging the unique capabilities of the femtosecond, picosecond and nanosecond laser beams from the XG-III laser facility.

The group successfully generated intense quasi-monoenergetic proton beams and quasi-static dense plasma samples. They performed high-precision experimental measurements of the stopping power of intense proton beams in dense plasma, demonstrating the Ohmic stopping mechanism, which plays a dominant role in extremely high-current beams^[143].

At the XG-III laser facility, the team developed experimental techniques for studying laser-accelerated heavy-ion beam interactions with dense matter. They obtained experimental data on the charge-state evolution of carbon ions in dense plasma using well-defined beam and target parameters, proving for the first time that target density effects increase the ion charge state near the critical density range^[144].

Using the XG-III laser, the group obtained the emission spectra of white dwarf-like matter. These emission lines provide critical data for identifying astro-observation spectra and determining the fundamental parameters of white dwarfs^[145].

The team demonstrated dynamic and unprecedented nanosecond-scale images of a flyer in a barrel. Advanced X-ray radiography, coupled with high-intensity laser

sources, enabled state-of-the-art radiographs in single-shot experiments^[146].

A relativistic intensity laser pulse with energies ranging from 25 to 130 J was used to produce strong magnetic fields in interaction with a specially designed no-hole capacitor-coil target. The magnetic field was estimated by proton deflectometry, ignoring the potential influence of the electric field. The maximum magnetic field obtained in the experiment at the center of the coil was 11,764 T^[147].

Proton radiography images of the interaction between an intense laser and NCD plasmas revealed various nonlinear plasma structures, such as ‘post-solitons’ in the plasma ‘hohlraum’^[148,149].

The group also reported on an experimental investigation of a laser–gas–converter approach for generating high-yield ultrashort MeV positrons. They observed that MeV electrons with high charges of several tens of nanocoulombs can be generated by an approximately 6 J, 40 fs laser pulse interacting with a high-density gas jet^[150].

3. Conclusion

This study provides an overview of high-intensity lasers with peak powers exceeding 100 TW, as well as associated research activities in China. Beyond the mentioned facilities, there is another 200 TW fs laser facility under construction at the Northwest Institute of Nuclear Technology (NINT), which is not addressed in detail. Numerous facilities

Table 5. Typical ultrafast high-intensity (> 100 TW) and nanosecond high-energy laser facilities in China.

	In commission	Under construction
>100 TW ultrafast high-intensity lasers	<ul style="list-style-type: none"> ➤ IOP 1 PW+3 TW ➤ CIAE 100 TW ➤ PKU 200 TW ➤ SJTU LLP 200 TW ➤ SIOM NLHPLP SG-II 5 PW ➤ SIOM LHFLP 200 TW; SULF 10 PW ➤ CAEP LFRC XG-III (fs+ps+ns); SILEX-II 5 PW 	<ul style="list-style-type: none"> ➤ PKU 2 PW+200 TW ➤ BAQIS-THU 1 PW ➤ THU-Fudan 300 TW ➤ SJTU LLP 200 TW+300 TW ➤ SJTU TDLI 2.5 PW ➤ SIOM SEL 100 PW ➤ SZTU 200 TW ➤ NUDT 200 TW ➤ NINT 200 TW
Nanosecond high-energy lasers	<ul style="list-style-type: none"> ➤ SG-II 2 kJ/ns/3ω ➤ SG-II UP 25 kJ/ns/3ω+2 PW/ps ➤ CAEP 100 kJ-level/ns/3ω 	

Notes: (1) The symbol ‘+’ denotes synchronous operation of the laser beams. (2) The data are sourced from public publications and private communications.

operating below 100 TW and high-repetition-rate ultrafast facilities focused on ultrafast dynamics and attosecond sciences are not covered, despite the ultrafast community being more extensive than the ultra-intense laser and high-energy-density physics communities.

Table 5 summarizes ultrafast high-intensity lasers exceeding 100 TW and nanosecond high-energy lasers at the kJ level, which are either operational or under construction in China, based on information from public publications and private communications.

The laser systems listed in the table include both standalone facilities and integrated combinations of different laser types (fs, ps or ns) that together form comprehensive research infrastructures. These facilities and platforms are primarily used to investigate scientific issues across two distinct domains. The first domain encompasses high-energy-density physics, including laser–plasma interactions, laser fusion, laboratory astrophysics, laser nuclear physics, novel laser-driven particle acceleration, ultrafast radiation sources ranging from X-rays to terahertz, high-energy physics, QED and other frontier problems. The second domain involves employing innovative laser-driven particles and radiation sources for interdisciplinary research in fields such as materials science, biology, chemistry and medicine. Some of these facilities have been designated as user facilities. Given that typical laser-driven secondary sources possess ultrafast properties and are capable of integration and synchronization, they are powerful tools for dynamic studies across various disciplines.

In addition to lasers with high peak power, there is a growing demand for lasers featuring high repetition rates and high average power, coupled with greater efficiency, to address a range of interdisciplinary scientific and industrial applications. These include the study of ultrafast dynamics in matter and applications in ultrafast biology, chemistry and therapeutics. Furthermore, the advancement of inertial fusion energy (IFE) research, spurred by the successful ICF ignition demonstration at the NIF in the United States, necessitates the development of new lasers. These lasers should offer not only high pulse energies but also the capability for high repetition rates. However, these topics are beyond the scope of the present paper.

The field of intense lasers and their applications is rapidly growing in China, with new laser facilities continuously under construction. This expansion provides more opportunities for cutting-edge scientific research and the advancement of various applications.

Acknowledgements

The authors express their gratitude to all Chinese colleagues who have made contributions to this paper without being listed as coauthors. We extend our apologies for any over-

sight or misrepresentation of facilities, and for those that may not have been included in this paper.

References

1. G. H. Miller, E. I. Moses, and C. R. Wuest, *Opt. Eng.* **443**, 2841 (2004).
2. D. Strickland and G. Mourou, *Opt. Commun.* **56**, 219 (1985).
3. W. Zheng, X. Wei, Q. Zhu, F. Jing, D. Hu, J. Su, K. Zheng, X. Yuan, H. Zhou, W. Dai, W. Zhou, F. Wang, D. Xu, X. Xie, B. Feng, Z. Peng, L. Guo, Y. Chen, X. Zhang, L. Liu, D. Lin, Z. Dang, Y. Xiang, and X. Deng, *High Power Laser Sci. Eng.* **4**, e21 (2016).
4. P. Zhang, J. T. He, D. B. Chen, Z. H. Li, Y. Zhang, J. G. Bian, L. Wang, Z. L. Li, B. H. Feng, X. L. Zhang, D. X. Zhang, X. W. Tang, and J. Zhang, *Phys. Rev. E* **57**, R3746 (1998).
5. L. M. Chen, J. Zhang, Y. T. Li, H. Teng, T. J. Liang, Z. M. Sheng, Q. L. Dong, L. Z. Zhao, Z. Y. Wei, and X. W. Tang, *Phys. Rev. Lett.* **87**, 225001 (2001).
6. Y. T. Li, J. Zhang, Z. M. Sheng, H. Teng, T. J. Liang, X. Y. Peng, X. Lu, Y. J. Li, and X. W. Tang, *Phys. Rev. Lett.* **90**, 165002 (2003).
7. Z. Y. Wei, J. Zhang, J. F. Xia, B. H. Feng, X. L. Zhang, and Y. Qiu, *Sci. China Ser. A Math.* **30**, 1046 (2001).
8. Z. H. Wang, Z. Y. Wei, W. J. Lin, P. Wang, H. Teng, J. R. Tian, J. Zhang, and J. Zhang, *J. Phys. IV France* **133**, 691 (2006).
9. Z. Wang, C. Liu, Z. Shen, Q. Zhang, H. Teng, and Z. Wei, *Opt. Lett.* **36**, 16 (2011).
10. Y. T. Li, X. H. Yuan, M. H. Xu, Z. Y. Zheng, Z. M. Sheng, M. Chen, Y. Y. Ma, W. X. Liang, Q. Z. Yu, Y. Zhang, F. Liu, Z. H. Wang, Z. Y. Wei, W. Zhao, Z. Jin, and J. Zhang, *Phys. Rev. Lett.* **96**, 165003 (2006).
11. W. M. Wang, P. Gibbon, Z. M. Sheng, Y. T. Li, and J. Zhang, *arXiv:1606.02437* (2016).
12. B. J. Zhu, Y. T. Li, D. W. Yuan, Y. F. Li, F. Li, G. Q. Liao, J. R. Zhao, J. Y. Zhong, F. B. Xue, S. K. He, W. W. Wang, F. Lu, F. Q. Zhang, L. Yang, K. N. Zhou, N. Xie, W. Hong, H. G. Wei, K. Zhang, B. Han, X. X. Pei, C. Liu, Z. Zhang, W. M. Wang, J. Q. Zhu, Y. Q. Gu, Z. Q. Zhao, B. H. Zhang, G. Zhao, and J. Zhang, *Appl. Phys. Lett.* **107**, 261903 (2015).
13. S. Fujioka, Z. Zhang, K. Ishihara, K. Shigemori, Y. Hironaka, T. Johzaki, A. Sunahara, N. Yamamoto, H. Nakashima, T. Watanabe, H. Shiraga, H. Nishimura, and H. Azechi, *Sci. Rep.* **3**, 1170 (2013).
14. Z. Zhang, B. Zhu, Y. Li, W. Jiang, D. Yuan, H. Wei, G. Liang, F. Wang, G. Zhao, J. Zhong, B. Han, N. Hua, B. Zhu, J. Zhu, C. Wang, Z. Fang, and J. Zhang, *High Power Laser Sci. Eng.* **6**, e38 (2018).
15. J. Zhang, W. M. Wang, X. H. Yang, D. Wu, Y. Y. Ma, J. L. Jiao, Z. Zhang, F. Y. Wu, X. H. Yuan, Y. T. Li, and J. Q. Zhu, *Philos. Trans. R. Soc. A* **378**, 20200015 (2020).
16. Z. Zhang, X.-H. Yuan, Y.-H. Zhang, H. Liu, K. Fang, C.-L. Zhang, Z.-D. Liu, X. Zhao, Q.-L. Dong, G.-Y. Liu, Y. Dai, H.-C. Gu, Y.-T. Li, J. Zheng, J.-Y. Zhong, and J. Zhang, *Acta Physica Sinica* **71**, 155201 (2022).
17. G. Q. Liao, Y. T. Li, C. Li, H. Liu, Y. H. Zhang, W. M. Jiang, X. H. Yuan, J. Nilsen, T. Ozaki, W. M. Wang, Z. M. Sheng, D. Neely, P. McKenna, and J. Zhang, *Plasma Phys. Control. Fusion* **59**, 014039 (2017).
18. G.-Q. Liao, Y.-T. Li, Y.-H. Zhang, H. Liu, X.-L. Ge, S. Yang, W.-Q. Wei, X.-H. Yuan, Y.-Q. Deng, B.-J. Zhu, Z. Zhang, W.-M. Wang, Z.-M. Sheng, L.-M. Chen, X. Lu, J.-L. Ma, X. Wang, and J. Zhang, *Phys. Rev. Lett.* **116**, 205003 (2016).

19. G. Liao, Y. Li, H. Liu, G. G. Scott, D. Neely, Y. Zhang, B. Zhu, Z. Zhang, C. Armstrong, E. Zemaityte, P. Bradford, P. G. Huggard, D. R. Rusby, P. McKenna, C. M. Brenner, N. C. Woolsey, W. Wang, Z. Sheng, and J. Zhang, *PNAS* **116**, 3994 (2019).
20. G.-Q. Liao, H. Liu, G. G. Scott, Y.-H. Zhang, B.-J. Zhu, Z. Zhang, Y.-T. Li, C. Armstrong, E. Zemaityte, P. Bradford, D. R. Rusby, D. Neely, P. G. Huggard, P. McKenna, C. M. Brenner, N. C. Woolsey, W.-M. Wang, Z.-M. Sheng, and J. Zhang, *Phys. Rev. X* **10**, 031062 (2020).
21. G. Liao, F. Sun, H. Lei, T. Wang, D. Wang, Y. Wei, F. Liu, X. Wang, Y. Li, and J. Zhang, *Phys. Rev. Lett.* **132**, 155001 (2024).
22. J. Zhong, Y. Li, X. Wang, J. Wang, Q. Dong, C. Xiao, S. Wang, X. Liu, L. Zhang, L. An, F. Wang, J. Zhu, Y. Gu, X. He, G. Zhao, and J. Zhang, *Nat. Phys.* **6**, 984 (2010).
23. Y. Ping, J. Zhong, X. Wang, B. Han, W. Sun, Y. Zhang, D. Yuan, C. Xing, J. Wang, Z. Liu, Z. Zhang, B. Qiao, H. Zhang, Y. Li, J. Zhu, G. Zhao, and J. Zhang, *Nat. Phys.* **19**, 263 (2023).
24. X. Liu, Y. T. Li, Y. Zhang, J. Y. Zhong, W. D. Zheng, Q. L. Dong, M. Chen, G. Zhao, Y. Sakawa, T. Morita, Y. Kuramitsu, T. N. Kato, L. M. Chen, X. Lu, J. L. Ma, W. M. Wang, Z. M. Sheng, H. Takabe, Y.-J. Rhee, Y. K. Ding, S. E. Jiang, S. Y. Liu, J. Q. Zhu, and J. Zhang, *New J. Phys.* **13**, 093001 (2011).
25. Z. Wang, C. He, B. Zhao, Z. Gao, J. Zhang, B. Tian, X. Xi, J. Li, C. Lyu, X. Meng, Q. Liu, X. Ban, F. Hu, X. Zhang, Y. Xu, S. Zhang, T. Ma, F. Liu, J. Lu, Z. Lu, H. Zhang, Y. Li, Y. Xiang, L. Wang, J. Liang, H. Dai, H. Wang, B. Guo, X. Jiang, and N. Wang, *Atom. Energy Sci. Technol.* **54**, 47 (2020).
26. B. Zhao, X. Zhang, C. Lv, Q. Liu, J. Zhang, X. Meng, M. Ma, and G. Yang, *Appl. Sci.* **12**, 5521 (2022).
27. B. Zhao, X. Zhang, C. Lv, Q. Liu, J. Zhang, M. Ma, and G. Yang, *AIP Adv.* **12**, 055128 (2022).
28. N. Wang, *Physics* **37**, 621 (2008).
29. Q. Liu, M. Ma, X. Zhang, B. Zhao, C. Lv, X. Meng, Z. Wang, C. He, B. Tian, X. Xi, F. Liu, and B. Guo, *AIP Adv.* **11**, 015145 (2021).
30. Q.-S. Liu, M.-J. Ma, B.-Z. Zhao, X.-H. Zhang, C. Lv, X.-H. Meng, J. Zhang, X.-N. Ban, Z. Wang, X.-F. Xi, B.-X. Tian, C.-Y. He, and B. Guo, *Nucl. Sci. Technol.* **32**, 75 (2021).
31. H.-R. Wang, B.-X. Tian, N. Bo, F.-L. Liu, C.-Y. He, S.-Q. Jia, B. Guo, and N.-Y. Wang, *Acta Phys. Sin.* **72**, 165201 (2023).
32. C. Lv, B.-Z. Zhao, F. Wan, H.-B. Cai, X.-H. Meng, B.-S. Xie, F.-L. Liu, Q.-S. Liu, X.-H. Zhang, J. Zhang, and Y.-C. Li, *Phys. Plasmas* **26**, 103101 (2019).
33. C. Lv, X.-H. Meng, Z. Wang, L.-H. Cao, F. Wan, Q.-S. Liu, X.-H. Zhang, and B.-Z. Zhao, *Phys. Plasmas* **27**, 063107 (2020).
34. Y. Yang, C. Lv, W. Sun, X. Ban, Q. Liu, Z. Deng, W. Qi, G. Yang, X. Zhang, F. Wan, Z. Wang, B. Zhao, J. Li, and W. Zhou, *Front. Phys.* **11**, 1189755 (2023).
35. J. Zhang, X. Ban, F. Wan, and C. Lv, *Appl. Sci.* **12**, 4464 (2022).
36. C. Lv, W. Sun, X. Ban, F. Wan, and Z. Wang, *Front. Phys.* **10**, 998583 (2022).
37. G. Yang, W. Sun, F. Wan, X. Ban, Q. Liu, Z. Wang, X. Zhang, M. Ma, J. Zhang, B. Zhao, and C. Lv, *Eur. Phys. J. D* **76**, 189 (2022).
38. X. Xi, B. Guo, C. Fu, C. Lyu, and G. Zhang, *Atom. Energy Sci. Technol.* **57**, 865 (2023).
39. X. Xi, G. Zhang, F. Liu, G. Fu, C. He, H. Chen, C. Lv, W. Sun, K. Zhang, P. Wang, X. Deng, Z. Ma, C. Fu, and B. Guo, *Rev. Sci. Instrum.* **94**, 013301 (2023).
40. H. Daido, M. Nishiuchi, and A. S. Pirozhkov, *Rep. Prog. Phys.* **75**, 056401 (2012).
41. A. Macchi, M. Borghesi, and M. Passoni, *Rev. Mod. Phys.* **85**, 751 (2013).
42. J. G. Zhu, M. J. Wu, Q. Liao, Y. X. Geng, K. Zhu, C. C. Li, X. H. Xu, D. Y. Li, Y. R. Shou, T. Yang, P. J. Wang, D. H. Wang, J. J. Wang, C. E. Chen, X. T. He, Y. Y. Zhao, W. J. Ma, H. Y. Lu, T. Tajima, C. Lin, and X. Q. Yan, *Phys. Rev. Accel. Beams* **22**, 061302 (2019).
43. Y. X. Geng, D. Wu, W. Yu, Z. M. Sheng, S. Fritzsche, Q. Liao, M. J. Wu, X. H. Xu, D. Y. Li, W. J. Ma, H. Y. Lu, Y. Y. Zhao, X. T. He, J. E. Chen, C. Lin, and X. Q. Yan, *Matter Radiat. Extrem* **5**, 064402 (2020).
44. Z. S. Mei, Z. Pan, Z. P. Liu, S. R. Xu, Y. R. Shou, P. J. Wang, Z. X. Cao, D. F. Kong, Y. L. Liang, Z. Y. Peng, T. Song, X. Chen, T. Q. Xu, Y. Gao, S. Y. Chen, J. R. Zhao, Y. Y. Zhao, X. Q. Yan, and W. J. Ma, *Phys. Plasmas* **30**, 033107 (2023).
45. J. Han, Z. Mei, C. Lu, J. Qian, Y. Liang, X. Sun, Z. Pan, D. Kong, S. Xu, Z. Liu, Y. Gao, G. Qi, Y. Shou, S. Chen, Z. Cao, Y. Zhao, C. Lin, Y. Zhao, Y. Geng, J. Chen, X. Yan, W. Ma, and G. Yang, *Front. Cell Dev. Biol.* **9**, 672929 (2021).
46. G. Yang, C. Lu, Z. Mei, X. Sun, J. Han, J. Qian, Y. Liang, Z. Pan, D. Kong, S. Xu, Z. Liu, Y. Gao, G. Qi, Y. Shou, S. Chen, Z. Cao, Y. Zhao, C. Lin, Y. Zhao, Y. Geng, W. Ma, and X. Yan, *Front. Cell Dev. Biol.* **9**, 672693 (2021).
47. D. Li, T. Yang, M. Wu, Z. Mei, K. Wang, C. Lu, Y. Zhao, W. Ma, K. Zhu, Y. Geng, G. Yang, C. Xiao, J. Chen, C. Lin, T. Tajima, and X. Yan, *Photonics* **10**, 132 (2023).
48. I. J. Kim, K. H. Pae, I. W. Choi, C. L. Lee, H. T. Kim, H. Singhal, J. H. Sung, S. K. Lee, H. W. Lee, P. V. Nickles, T. M. Jeong, C. M. Kim, and C. H. Nam, *Phys. Plasmas* **23**, 6 (2016).
49. A. Higginson, R. J. Gray, M. King, R. J. Dance, S. D. R. Williamson, N. M. H. Butler, R. Wilson, R. Capdessus, C. Armstrong, J. S. Green, S. J. Hawkes, P. Martin, W. Q. Wei, S. R. Mirfayzi, X. H. Yuan, S. Kar, M. Borghesi, R. J. Clarke, D. Neely, and P. McKenna, *Nat. Commun.* **9**, 724 (2018).
50. W. J. Ma, I. J. Kim, J. Q. Yu, I. W. Choi, P. K. Singh, H. W. Lee, J. H. Sung, S. K. Lee, C. Lin, Q. Liao, J. G. Zhu, H. Y. Lu, B. Liu, H. Y. Wang, R. F. Xu, X. T. He, J. E. Chen, M. Zepf, J. Schreiber, X. Q. Yan, and C. H. Nam, *Phys. Rev. Lett.* **122**, 014803 (2019).
51. W. J. Ma, Z. P. Liu, P. J. Wang, J. R. Zhao, and X. Q. Yan, *Acta Phys. Sin.* **70**, 15 (2021).
52. J. Schreiber, P. R. Bolton, and K. Parodi, *Rev. Sci. Instrum.* **87**, 071101 (2016).
53. P. J. Wang, Z. Gong, S. G. Lee, Y. R. Shou, Y. X. Geng, C. Jeon, I. J. Kim, H. W. Lee, J. W. Yoon, J. H. Sung, S. K. Lee, D. F. Kong, J. B. Liu, Z. S. Mei, Z. X. Cao, Z. Pan, I. W. Choi, X. Q. Yan, C. H. Nam, and W. J. Ma, *Phys. Rev. X* **11**, 021049 (2021).
54. Z. X. Cao, Z. Y. Peng, Y. R. Shou, J. R. Zhao, S. Y. Chen, Y. Gao, J. B. Liu, P. J. Wang, Z. S. Mei, Z. Pan, D. F. Kong, G. J. Qi, S. R. Xu, Z. P. Liu, Y. L. Liang, S. X. Xu, T. Song, X. Chen, Q. F. Wu, X. Liu, and W. J. Ma, *Front. Phys.* **11**, 1172075 (2023).
55. Y. R. Shou, P. J. Wang, S. G. Lee, Y. J. Rhee, H. W. Lee, J. W. Yoon, J. H. Sung, S. K. Lee, Z. Pan, D. F. Kong, Z. S. Mei, J. B. Liu, S. R. Xu, Z. G. Deng, W. M. Zhou, T. Tajima, I. Choi, X. Q. Yan, C. H. Nam, and W. J. Ma, *Nat. Photonics* **17**, 137 (2023).
56. W. Ma, *Nano Res.* **16**, 12572 (2023).
57. J. H. Bin, M. Yeung, Z. Gong, H. Y. Wang, C. Kreuzer, M. L. Zhou, M. J. V. Streeter, P. S. Foster, S. Cousens, B. Dromey, J. Meyer-Ter-Vehn, M. Zepf, and J. Schreiber, *Phys. Rev. Lett.* **120**, 074801 (2018).

58. J. H. Bin, W. J. Ma, H. Y. Wang, M. J. V. Streeter, C. Kreuzer, D. Kiefer, M. Yeung, S. Cousens, P. S. Foster, B. Dromey, X. Q. Yan, R. Ramis, J. Meyer-ter-Vehn, M. Zepf, and J. Schreiber, *Phys. Rev. Lett.* **115**, 064801 (2015).
59. K. D. Wang, K. Zhu, M. J. Easton, Y. J. Li, C. Lin, and X. Q. Yan, *Phys. Rev. Accel. Beams* **23**, 110001 (2020).
60. Y. P. Wu, J. F. Hua, Z. Zhou, J. Zhang, S. Liu, B. Peng, Y. Fang, Z. Nie, X. N. Ning, C.-H. Pai, Y. C. Du, W. Lu, C. J. Zhang, W. B. Mori, and C. Joshi, *Phys. Rev. Lett.* **122**, 204804 (2019).
61. Y. Wu, J. Hua, C.-H. Pai, and W. An, *Phys. Rev. Appl.* **12**, 64011 (2019).
62. X. L. Xu, J. F. Hua, F. Li, C. J. Zhang, L. X. Yan, Y. C. Du, W. H. Huang, H. B. Chen, C. X. Tang, W. Lu, P. Yu, W. An, C. Joshi, and W. B. Mori, *Phys. Rev. Lett.* **112**, 035003 (2014).
63. X. L. Xu, J. F. Hua, Y. P. Wu, C. J. Zhang, F. Li, Y. Wan, C.-H. Pai, W. Lu, W. An, P. Yu, M. J. Hogan, C. Joshi, and W. B. Mori, *Phys. Rev. Lett.* **116**, 024801 (2016).
64. X. L. Xu, Y. P. Wu, C. J. Zhang, F. Li, Y. Wan, J. F. Hua, C.-H. Pai, W. Lu, P. Yu, C. Joshi, and W. B. Mori, *Phys. Rev. Spec. Top. Accel. Beams* **17**, 061301 (2014).
65. X. L. Xu, F. Li, W. An, T. N. Dalichaouch, P. Yu, W. Lu, C. Joshi, and W. B. Mori, *Phys. Rev. Accel. Beams* **20**, 111303 (2017).
66. F. Li, J. F. Hua, X. L. Xu, C. J. Zhang, L. X. Yan, Y. C. Du, W. H. Huang, H. B. Chen, C. X. Tang, W. Lu, C. Joshi, W. B. Mori, and Y. Q. Gu, *Phys. Rev. Lett.* **111**, 015003 (2013).
67. F. Li, T. N. Dalichaouch, J. R. Pierce, X. Xu, F. S. Tsung, W. Lu, C. Joshi, and W. B. Mori, *Phys. Rev. Lett.* **128**, 174803 (2022).
68. C. J. Zhang, J. F. Hua, X. L. Xu, F. Li, C.-H. Pai, Y. Wan, Y. P. Wu, Y. Q. Gu, W. B. Mori, C. Joshi, and W. Lu, *Sci. Rep.* **6**, 29485 (2016).
69. C. J. Zhang, J. F. Hua, Y. Wan, C.-H. Pai, B. Guo, J. Zhang, Y. Ma, F. Li, Y. P. Wu, H.-H. Chu, Y. Q. Gu, X. L. Xu, W. B. Mori, C. Joshi, J. Wang, and W. Lu, *Phys. Rev. Lett.* **119**, 064801 (2017).
70. S. Zhou, J. Hua, W. An, W. B. Mori, C. Joshi, J. Gao, and W. Lu, *Phys. Rev. Lett.* **127**, 174801 (2021).
71. S. Zhou, J. Hua, W. Lu, W. An, Q. Su, W. B. Mori, and C. Joshi, *Phys. Rev. Accel. Beams* **25**, 091303 (2022).
72. Y. Wu, J. Hua, Z. Zhou, J. Zhang, S. Liu, B. Peng, Y. Fang, X. Ning, Z. Nie, F. Li, C. Zhang, C.-H. Pai, Y. Du, W. Lu, W. B. Mori, and C. Joshi, *Nat. Phys.* **17**, 801 (2021).
73. Y. Xia, Q. Wang, J. Zhao, L. Feng, E. Guo, T. Yang, Y. Wang, F. Li, Z. Guo, Q. He, K. Chen, Y. Lu, X. Yan, and C. Lin, *IEEE Trans. Nucl. Sci.* **71**, 18 (2024).
74. Y. Ma, J. Hua, D. Liu, Y. He, T. Zhang, J. Chen, F. Yang, X. Ning, Z. Yang, J. Zhang, C.-H. Pai, Y. Gu, and W. Lu, *Matter Radiat. Extremes* **5**, 064401 (2020).
75. B. Guo, Z. Cheng, S. Liu, X. N. Ning, J. Zhang, C. H. Pai, J. F. Hua, H. H. Chu, J. Wang, and W. Lu, *Plasma Phys. Control. Fusion* **61**, 035003 (2019).
76. Y. Ma, J. Hua, D. Liu, Y. He, T. Zhang, J. Chen, F. Yang, X. Ning, H. Zhang, Y. Du, and W. Lu, *Phys. Rev. Appl.* **19**, 014073 (2023).
77. B. Guo, X. Zhang, J. Zhang, J. Hua, C.-H. Pai, C. Zhang, H.-H. Chu, W. Mori, C. Joshi, J. Wang, and W. Lu, *Sci. Rep.* **9**, 7796 (2019).
78. Z. Nie, C.-H. Pai, J. Hua, C. Zhang, Y. Wu, Y. Wan, F. Li, J. Zhang, Z. Cheng, Q. Su, S. Liu, Y. Ma, X. Ning, Y. He, W. Lu, H.-H. Chu, J. Wang, W. B. Mori, and C. Joshi, *Nat. Photonics* **12**, 489 (2018).
79. Z. Nie, C.-H. Pai, J. Zhang, X. Ning, J. Hua, Y. He, Y. Wu, Q. Su, S. Liu, Y. Ma, Z. Cheng, W. Lu, H.-H. Chu, J. Wang, C. Zhang, W. B. Mori, and C. Joshi, *Nat. Commun.* **11**, 2787 (2020).
80. Y. Fang, F. Li, J. Hua, B. Guo, L. Zhou, B. Zhou, Z. Chen, J. Liu, Z. Zhou, Y. Wu, Y. Du, R. Li, and W. Lu, [arXiv:2210.12093](https://arxiv.org/abs/2210.12093) (2022).
81. Y. Wan, I. A. Andriyash, W. Lu, W. B. Mori, and V. Malka, *Phys. Rev. Lett.* **125**, 104801 (2020).
82. Y. Wan, I. A. Andriyash, C. H. Pai, J. F. Hua, C. J. Zhang, F. Li, Y. P. Wu, Z. Nie, W. B. Mori, and W. Lu, *New J. Phys.* **22**, 052002 (2020).
83. X. Ge, X. Yuan, Y. Fang, W. Wei, S. Yang, F. Liu, M. Chen, L. Zhao, Z. Sheng, and J. Zhang, *Chin. Opt. Lett.* **16**, 103202 (2018).
84. M. Zeng, M. Chen, Z.-M. Sheng, W. B. Mori, and J. Zhang, *Phys. Plasmas* **21**, 030701 (2014).
85. M. Zeng, M. Chen, L. L. Yu, W. B. Mori, Z. M. Sheng, B. Hidding, D. A. Jaroszynski, and J. Zhang, *Phys. Rev. Lett.* **114**, 084801 (2015).
86. M. Mirzaie, S. Li, M. Zeng, N. Hafz, M. Chen, G. Li, Q. Zhu, H. Liao, T. Sokollik, F. Liu, Y. Ma, L. Chen, Z. Sheng, and J. Zhang, *Sci. Rep.* **5**, 14659 (2015).
87. S. Li, G. Li, Q. Ain, M. S. Hur, A. C. Ting, V. V. Kulagin, C. Kamperidis, N. A. M. Hafz, *Sci. Adv.* **5**, eaav7940 (2019).
88. J. Luo, M. Chen, W. Y. Wu, S. M. Weng, Z. M. Sheng, C. B. Schroeder, D. A. Jaroszynski, E. Esarey, W. P. Leemans, W. B. Mori, and J. Zhang, *Phys. Rev. Lett.* **120**, 154801 (2018).
89. X. Zhu, B. Li, F. Liu, J. Li, Z. Bi, X. Ge, H. Deng, Z. Zhang, P. Cui, L. Lu, W. Yan, X. Yuan, L. Chen, Q. Cao, Z. Liu, Z. Sheng, M. Chen, and J. Zhang, *Phys. Rev. Lett.* **130**, 215001 (2023).
90. L. Wang, Z. Zhang, S. Chen, Y. Chen, X. Hu, M. Zhu, W. Yan, H. Xu, L. Sun, M. Chen, F. Liu, L. Chen, J. Zhang, and Z. Sheng, *Phys. Rev. Lett.* **132**, 165002 (2024).
91. B. Y. Li, F. Liu, M. Chen, F. Y. Wu, J. W. Wang, L. Lu, J. L. Li, X. L. Ge, X. H. Yuan, W. C. Yan, L. M. Chen, Z. M. Sheng, and J. Zhang, *Phys. Rev. Lett.* **128**, 244801 (2022).
92. B. Y. Li, F. Liu, M. Chen, Z. Y. Chen, X. H. Yuan, S. M. Weng, T. Jin, S. G. Rykovanov, J. W. Wang, Z. M. Sheng, and J. Zhang, *Phys. Rev. E* **100**, 053207 (2019).
93. J. Feng, W. Wang, C. Fu, L. Chen, J. Tan, Y. Li, J. Wang, Y. Li, G. Zhang, Y. Ma, and J. Zhang, *Phys. Rev. Lett.* **128**, 052501 (2022).
94. J. Feng, Y. Li, J. Tan, W. Wang, Y. Li, X. Zhang, Y. Meng, X. Ge, F. Liu, W. Yan, C. Fu, L. Chen, and J. Zhang, *Laser Photonics Rev.* **17**, 2300514 (2023).
95. J. Zhu, J. Zhu, X. Li, B. Zhu, W. Ma, X. Lu, W. Fan, Z. Liu, S. Zhou, G. Xu, G. Zhang, X. Xie, L. Yang, J. Wang, X. Ouyang, L. Wang, D. Li, P. Yang, Q. Fan, M. Sun, C. Liu, D. Liu, Y. Zhang, H. Tao, M. Sun, P. Zhu, B. Wang, Z. Jiao, L. Ren, D. Liu, X. Jiao, H. Huang, and Z. Lin, *High Power Laser Sci. Eng.* **6**, e55 (2018).
96. J. Zhu, X. Xie, M. Sun, J. Kang, Q. Yang, A. Guo, H. Zhu, P. Zhu, Q. Gao, X. Liang, Z. Cui, S. Yang, C. Zhang, and Z. Lin, *High Power Laser Sci. Eng.* **6**, e29 (2018).
97. G. Xu, T. Wang, Z. Li, Y.-p. Dai, Z. Lin, Y. Y. Gu, and J. Zhu, *Rev. Laser Eng.* **36**, 1172 (2008).
98. Q. Yang, A. Guo, X. Xie, F. Zhang, M. Sun, Q. Gao, M. Li, and Z. Lin, *Optik* **121**, 696 (2010).
99. H. H. An, W. Wang, J. Xiong, C. Wang, X. Pan, X. P. Ouyang, S. Jiang, Z. Y. Xie, P. P. Wang, Y. L. Yao, N. Hua, Y. Wang, Z. C. Jiang, Q. Xiao, F. C. Ding, Y. T. Wan, X. Liu, R. R. Wang, Z. H. Fang, P. Q. Yang, Y. E. Jiang, P. Z. Zhang, B. Q. Zhu, J. R. Sun, B. Qiao, A. L. Lei, and J. Q. Zhu, *High Power Laser Sci. Eng.* **11**, e63 (2023).
100. F. Zhang, H. B. Cai, W. M. Zhou, Z. S. Dai, L. Q. Shan, H. Xu, J. B. Chen, F. J. Ge, Q. Tang, W. S. Zhang, L. Wei, D. X. Liu, J. F. Gu, H. B. Du, B. Bi, S. Z. Wu, J. Li, F. Lu, H.

- Zhang, B. Zhang, M. Q. He, M. H. Yu, Z. H. Yang, W. W. Wang, H. S. Zhang, B. Cui, L. Yang, J. F. Wu, W. Qi, L. H. Cao, Z. Li, H. J. Liu, Y. M. Yang, G. L. Ren, C. Tian, Z. Q. Yuan, W. D. Zheng, L. F. Cao, C. T. Zhou, S. Y. Zou, Y. Q. Gu, K. Du, Y. K. Ding, B. H. Zhang, S. P. Zhu, W. Y. Zhang, and X. T. He, *Nat. Phys.* **16**, 810 (2020).
101. Y. Gu, F. Zhang, L. Shan, B. Bi, J. Chen, L. Wei, J. Li, Z. Song, Z. Liu, Z. Yang, M. Yu, B. Cui, Y. Zhang, H. Liu, D. Liu, W. Wang, Z. Dai, Y. Yang, L. Yang, F. Zhang, X. Wu, K. Du, W. Zhou, L. Cao, B. Zhang, J. Wu, G. Ren, H. Cai, S. Wu, L. Cao, H. Zhang, C. Zhou, and X. He, *High Power Laser Particle Beams* **27**, 110101 (2015).
 102. X. Liang, Y. Leng, C. Wang, C. Li, L. Lin, B. Zhao, Y. Jiang, X. Lu, M. Hu, C. Zhang, H. Lu, D. Yin, Y. Jiang, X. Lu, H. Wei, J. Zhu, R. Li, and Z. Xu, *Opt. Express* **15**, 15335 (2007).
 103. Y. Chu, X. Liang, L. Yu, Y. Xu, L. Xu, L. Ma, X. Lu, Y. Liu, Y. Leng, R. Li, and Z. Xu, *Opt. Express*, **21**, 29231 (2013).
 104. Y. Chu, Z. Gan, X. Liang, L. Yu, X. Lu, C. Wang, X. Wang, L. Xu, H. Lu, D. Yin, Y. Leng, R. Li, and Z. Xu, *Opt. Lett.* **40**, 5011 (2015).
 105. Y. Xu, J. Lu, W. Li, F. Wu, Y. Li, C. Wang, Z. Li, X. Lu, Y. Liu, Y. Leng, R. Li, and Z. Xu, *Opt. Laser Technol.* **79**, 141 (2016).
 106. W. Wang, K. Feng, L. Ke, C. Yu, Y. Xu, R. Qi, and Y. Chen, *Nature* **595**, 516 (2021).
 107. Z. Gan, L. Yu, S. Li, C. Wang, X. Liang, Y. Liu, W. Li, Z. Guo, Z. Fan, X. Yuan, L. Xu, Z. Liu, Y. Xu, J. Lu, H. Lu, D. Yin, Y. Leng, R. Li, and Z. Xu, *Opt. Express*, **25**, 5169 (2017).
 108. W. Li, Z. Gan, L. Yu, C. Wang, Y. Liu, Z. Guo, L. Xu, M. Xu, Y. Hang, Y. Xu, J. Wang, P. Huang, H. Cao, B. Yao, X. Zhang, L. Chen, Y. Tang, S. Li, X. Liu, S. Li, M. He, D. Yin, X. Liang, Y. Leng, R. Li, and Z. Xu, *Opt. Lett.* **43**, 5681 (2018).
 109. L. Yu, Y. Xu, Y. Liu, Y. Li, S. Li, Z. Liu, W. Li, F. Wu, X. Yang, Y. Yang, C. Wang, X. Lu, Y. Leng, R. Li, and Z. Xu, *Opt. Express* **26**, 2625 (2018).
 110. L. Yu, Y. Xu, S. Li, Y. Liu, J. Hu, F. Wu, X. Yang, Z. Zhang, Y. Wu, P. Bai, X. Wang, X. Lu, Y. Leng, R. Li, and Z. Xu, *Opt. Express* **27**, 8683 (2019).
 111. S. Li, C. Wang, Y. Liu, Y. Xu, Y. Li, X. Liu, Z. Gan, L. Yu, X. Liang, Y. Leng, and R. Li, *Opt. Express* **25**, 17488 (2017).
 112. Z. Zhang, F. Wu, J. Hu, X. Yang, J. Gui, P. Ji, X. Liu, C. Wang, Y. Liu, X. Lu, Y. Xu, Y. Leng, R. Li, and Z. Xu, *High Power Laser Sci. Eng.* **8**, e4 (2020).
 113. J. Gao, J. Wu, Z. Lou, F. Yang, J. Qian, Y. Peng, Y. Leng, Y. Zheng, Z. Zeng, and R. Li, *Optica* **9**, 1003 (2022).
 114. A. X. Li, C. Y. Qin, H. Zhang, S. Li, L. L. Fan, Q. S. Wang, T. J. Xu, N. W. Wang, L. H. Yu, Y. Xu, Y. Q. Liu, C. Wang, X. L. Wang, Z. X. Zhang, X. Y. Liu, P. L. Bai, Z. B. Gan, X. B. Zhang, X. B. Wang, C. Fan, Y. J. Sun, Y. H. Tang, B. Yao, X. Y. Liang, Y. X. Leng, B. F. Shen, L. L. Ji, R. X. Li, and Z. Z. Xu, *High Power Laser Sci. Eng.* **10**, e26 (2022).
 115. X. Wu, D. Kong, S. Hao, Y. Zeng, X. Yu, B. Zhang, M. Dai, S. Liu, J. Wang, Z. Ren, S. Chen, J. Sang, K. Wang, D. Zhang, Z. Liu, J. Gui, X. Yang, Y. Xu, Y. Leng, Y. Li, L. Song, Y. Tian, and R. Li, *Adv. Mater.* **35**, 2208947 (2023).
 116. Y. Peng, Y. Xu, L. Yu, X. Wang, Y. Li, X. Lu, C. Wang, J. Liu, C. Zhao, Y. Liu, C. Wang, X. Liang, Y. Leng, and R. Li, *Rev. Laser Eng.* **49**, 93 (2021).
 117. B. Shao, Y. Li, Y. Peng, P. Wang, J. Qian, Y. Leng, and R. Li, *Opt. Lett.* **45**, 2215 (2020).
 118. X. Wang, X. Liu, X. Lu, J. Chen, Y. Long, W. Li, H. Chen, X. Chen, P. Bai, Y. Li, Y. Peng, Y. Liu, F. Wu, C. Wang, Z. Li, Y. Xu, X. Liang, Y. Leng, and R. Li, *Ultrafast Sci.* **2022**, 9894358 (2022).
 119. C. Wang, D. Wang, Y. Xu, and Y. Leng, *Opt. Commun.* **507**, 127613 (2022).
 120. B. Shen, Z. Bu, J. Xu, T. Xu, L. Ji, R. Li, and Z. Xu, *Plasma Phys. Control. Fusion*. **60**, 044002 (2018).
 121. Y. Zhao, H. Y. Lu, C. T. Zhou, and J. G. Zhu, *Matter Radiat. Extremes* **8**, 14403 (2023).
 122. Y. Zhao, H. Y. Lu, C. T. Zhou, C. X. Zhang, M. H. Liao, H. L. Chen, Z. Y. Zou, M. C. Shang, and S. Y. Yin, *AIP Adv.* **13**, 35239 (2023).
 123. R. Li, T. W. Huang, L. B. Ju, M. Y. Yu, H. Zhang, S. Z. Wu, H. B. Zhuo, C. T. Zhou, and S. C. Ruan, *Phys. Rev. Lett.* **127**, 245002 (2021).
 124. K. Jiang, T. W. Huang, R. Li, M. Y. Yu, H. B. Zhuo, S. Z. Wu, C. T. Zhou, and S. C. Ruan, *Phys. Rev. Lett.* **130**, 185001 (2023).
 125. K. Jiang, T. W. Huang, R. Li, and C. T. Zhou, *Phys. Plasmas* **31**, 022303 (2024).
 126. H. Peng, T. W. Huang, K. Jiang, R. Li, C. N. Wu, M. Y. Yu, C. Riconda, S. Weber, C. T. Zhou, and S. C. Ruan, *Phys. Rev. Lett.* **131**, 145003 (2023).
 127. L. Li, J. C. P. Koliyadu, H. Donnelly, D. Alj, O. Delmas, M. Ruiz-Lopez, O. de La Rochefoucauld, G. Dovillaire, M. Fajardo, C. T. Zhou, S. Ruan, B. Dromey, M. Zepf, and P. Zeitoun, *Opt. Lett.* **45**, 4248 (2020).
 128. M. Ruiz-Lopez, M. Mehrjoo, B. Keitel, E. Plonjes, D. Alj, G. Dovillaire, L. Li, and P. Zeitoun, *Sensor* **20**, 6426 (2020).
 129. Y. Zhang, L. Li, L. F. Gan, S. P. Zhu, X. T. He, P. Zeitoun, and B. Qiao, *Phys. Rev. Appl.* **21**, 014058 (2024).
 130. C. Wu, L. Li, M. Yeung, S. Wu, S. Cousens, S. Tietze, B. Dromey, C. Zhou, S. Ruan, and M. Zepf, *Opt. Express* **20**, 389 (2022).
 131. D. Zhang, Z. Lü, C. Meng, X. Du, Z. Zhou, Z. Zhao, and J. Yuan, *Phys. Rev. Lett.* **109**, 243002 (2012).
 132. L. Zhihui, D. Zhang, C. Meng, L. Sun, Z. Zhou, Z. Zhao, and J. Yuan, *Appl. Phys. Lett.* **101**, 081119 (2012).
 133. X. Wang, L. Wang, F. Xiao, D. Zhang, Z. Lü, J. Yuan, and Z. Zhao, *Chin. Phys. Lett.* **37**, 023201 (2020).
 134. S. Luo, J. Liu, X. Li, D. Zhang, X. Yu, D. Ren, M. Li, Y. Yang, Z. Wang, P. Ma, C. Wang, J. Zhao, Z. Zhao, and D. Ding, *Phys. Rev. Lett.* **126**, 103202 (2021).
 135. H. Lei, J. Yao, J. Zhao, H. Xie, F. Zhang, H. Zhang, N. Zhang, G. Li, Q. Zhang, X. Wang, Y. Yang, L. Yuan, Y. Cheng, and Z. Zhao, *Nat. Commun.* **13**, 4080 (2022).
 136. L. Wang, G. Bai, X. Wang, J. Zhao, C. Gao, J. Wang, F. Xiao, W. Tao, P. Song, Q. Qiu, J. Liu, and Z. Zhao, *Nat. Commun.* **15**, 2705 (2024).
 137. J. Y. Dai, Y. Hou, and J. M. Yuan, *Phys. Rev. Lett.* **104**, 245001 (2010).
 138. Q. Zeng, B. Chen, X. Yu, S. Zhang, D. Kang, H. Wang, and J. Dai, *Phys. Rev. B* **105**, 174109 (2022).
 139. Q. Zeng, B. Chen, S. Zhang, D. Kang, H. Wang, X. Yu, and J. Dai, *npj Comput. Mater.* **9**, 213 (2023).
 140. H. S. Peng, X. J. Huang, Q. H. Zhu, X. D. Wang, K. N. Zhou, X. F. Wei, X. M. Zeng, L. Q. Liu, X. Wang, Y. Guo, D. H. Lin, B. Xu, L. B. Xu, X. L. Chu, and X. M. Zhang, *Laser Phys.* **16**, 244 (2006).
 141. Q. Zhu, K. Zhou, J. Su, N. Xie, X. Huang, X. Zeng, X. Wang, X. Wang, Y. Zuo, D. Jiang, L. Zhao, F. Li, D. Hu, K. Zheng, W. Dai, D. Chen, Z. Dang, L. Liu, D. Xu, D. Lin, X. Zhang, Y. Deng, X. Xie, B. Feng, Z. Peng, R. Zhao, F. Wang, W. Zhou, L. Sun, Y. Guo, S. Zhou, J. Wen, Z. Wu, Q. Li, Z. Huang, D. Wang, X. Jiang, Y. Gu, F. Jing, and B. Zhang, *Laser Phys. Lett.* **15**, 015301 (2018).
 142. N. Xie, K. Zhou, W. Huang, X. Wang, L. Sun, Y. Guo, and Q. Li, *Opt. Eng.* **51**, 024201 (2012).
 143. J. Ren, Z. Deng, W. Qi, B. Chen, B. Ma, X. Wang, S. Yin, J. Feng, W. Liu, Z. Xu, D. H. H. Hoffmann, S. Wang, Q. Fan, B. Cui, S. He, Z. Cao, Z. Zhao, L. Cao, Y. Gu, S. Zhu, R. Cheng, X. Zhou, G. Xiao, H. Zhao, Y. Zhang, Z. Zhang, Y.

- Li, D. Wu, W. Zhou, and Y. Zhao, *Nat. Commun.* **11**, 5157 (2020).
144. J. Ren, B. Ma, L. Liu, W. Wei, B. Chen, S. Zhang, H. Xu, Z. Hu, F. Li, X. Wang, S. Yin, J. Feng, X. Zhou, Y. Gao, Y. Li, X. Shi, J. Li, X. Ren, Z. Xu, Z. Deng, W. Qi, S. Wang, Q. Fan, B. Cui, W. Wang, Z. Yuan, J. Teng, Y. Wu, Z. Cao, Z. Zhao, Y. Gu, L. Cao, S. Zhu, R. Cheng, Y. Lei, Z. Wang, Z. Zhou, G. Xiao, H. Zhao, D. H. H. Hoffmann, W. Zhou, and Y. Zhao, *Phys. Rev. Lett.* **130**, 095101 (2023).
145. B.-B. Ma, J.-R. Ren, S.-Y. Wang, D. H. H. Hoffmann, Z.-G. Deng, W. Qi, X. Wang, S. Yin, J.-H. Feng, Q.-P. Fan, W. Liu, Z.-F. Xu, Y. Chen, B. Cui, S.-K. He, Z.-R. Cao, Z.-Q. Zhao, Y.-Q. Gu, S.-P. Zhu, R. Cheng, X.-M. Zhou, G.-Q. Xiao, H.-W. Zhao, Y.-H. Zhang, Z. Zhang, Y.-T. Li, X. Xu, W.-Q. Wei, B.-Z. Chen, S.-Z. Zhang, Z.-M. Hu, L.-R. Liu, F.-F. Li, H. Xu, W.-M. Zhou, L.-F. Cao, and Y.-T. Zhao, *Astrophys. J.* **920**, 106 (2021).
146. G.-B. Chu, Y. Wang, Y.-B. Yan, M.-B. Yu, M. Shui, F. Tan, D. Tang, W. Wang, L. Wang, B. He, and W.-M. Zhou, *Opt. Express* **32**, 9602 (2024).
147. W. Wang, L. Shan, F. Zhang, Z. Yuan, D. Liu, C. Tian, L. Yang, F. Lu, W. Qi, Z. Deng, K. Zhou, N. Xie, X. Wang, J. Mu, W. Zhou, H. Cai, S. Zhu, and Y. Gu, *Phys. Plasmas* **30**, 072703 (2023).
148. D. N. Yue, M. Chen, P. F. Geng, X. H. Yuan, Z. M. Sheng, J. Zhang, Q. L. Dong, A. Das, and G. R. Kumar, *Plasma Phys. Control. Fusion* **63**, 075009 (2021).
149. D. N. Yue, M. Chen, P. F. Geng, X. H. Yuan, Q. L. Dong, Z. M. Sheng, and J. Zhang, *Plasma Phys. Control. Fusion* **64**, 045025 (2022).
150. Z. M. Zhang, Y. C. Wu, X. H. Zhang, Y. H. Yan, H. Huang, L. B. Meng, W. Qi, B. Zhang, S. K. He, and B. Cui, *Plasma Phys. Control. Fusion* **64**, 095015 (2022).